US 20230051729A1

(19) **United States**
(12) **Patent Application Publication**
LIU
(10) **Pub. No.: US 2023/0051729 A1**
(43) **Pub. Date: Feb. 16, 2023**

(54) **PROCESS AND APPARATUS FOR CONTINUOUS PRODUCTION OF POROUS STRUCTURES**

(71) Applicant: **Molecule Works Inc.**, Richland, WA (US)

(72) Inventor: **Wei LIU**, Richland, WA (US)

(21) Appl. No.: **17/943,680**

(22) Filed: **Sep. 13, 2022**

Related U.S. Application Data

(62) Division of application No. 16/235,178, filed on Dec. 28, 2018, now Pat. No. 11,486,030.

(60) Provisional application No. 62/675,341, filed on May 23, 2018.

Publication Classification

(51) **Int. Cl.**

C23C 8/06	(2006.01)
B22F 3/10	(2006.01)
C23C 8/60	(2006.01)
C23C 16/30	(2006.01)
C23C 16/28	(2006.01)
C23C 8/02	(2006.01)

(52) **U.S. Cl.**

CPC ***C23C 8/06*** (2013.01); ***B22F 3/1039*** (2013.01); ***C23C 8/60*** (2013.01); ***C23C 16/30*** (2013.01); ***C23C 16/28*** (2013.01); ***C23C 8/02*** (2013.01); *B22F 3/1143* (2013.01)

(57) **ABSTRACT**

A method for producing metal-based micro-porous structures includes continuously feeding a solid green part and a gas flow into a tunnel reactor having an aspect ratio greater than 2, wherein the solid green part has a characteristic diffusion mass transfer dimension less than 1 mm and a gas in the gas flow is substantially free of oxidants, and chemically reacting the gas in the gas flow and the green part under a predetermined temperature profile along a length of the tunnel reactor for a sufficient time to convert the green part into a solid product having pore sizes in a range of 0.3 nm to 5 μm.

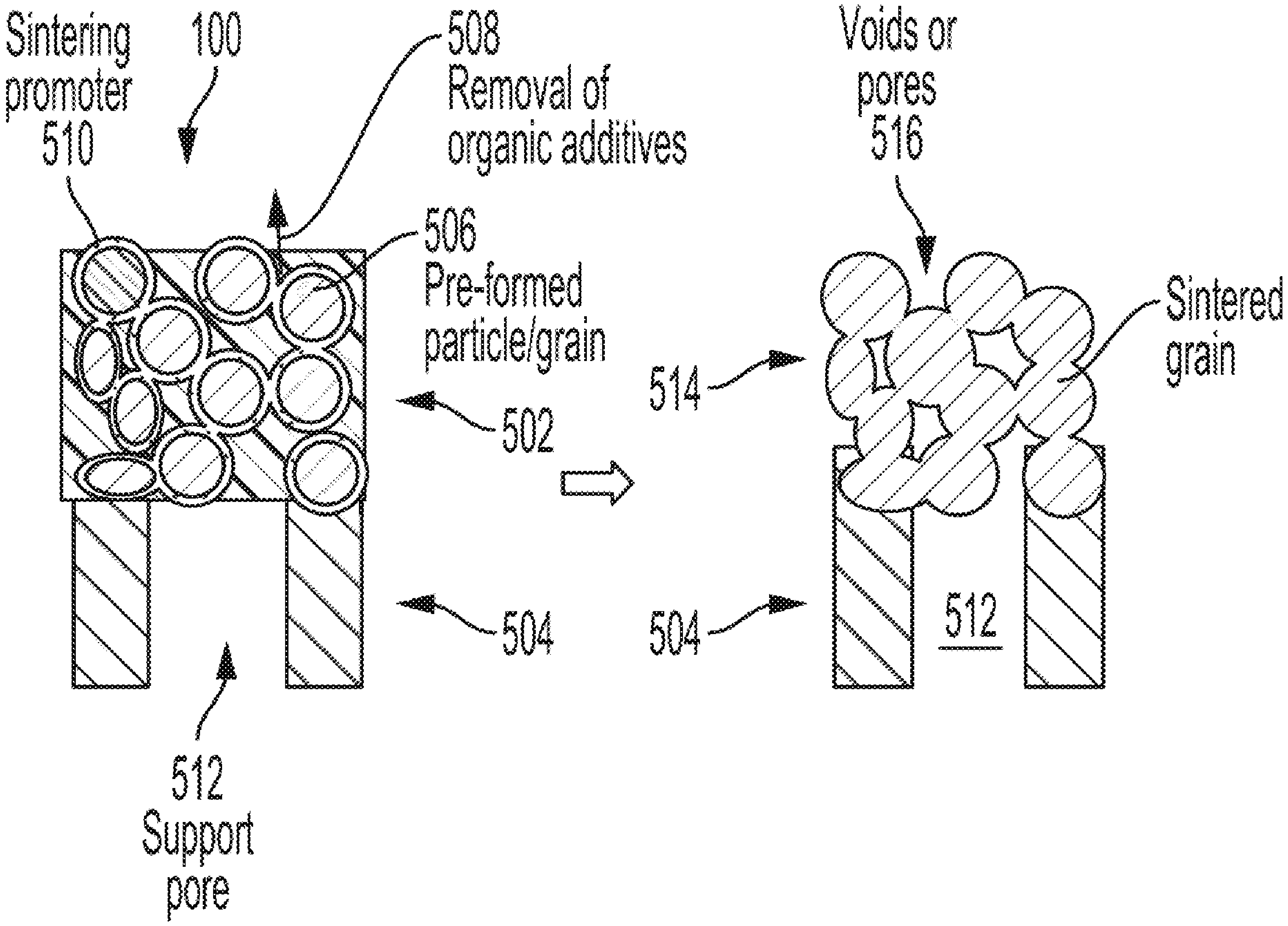

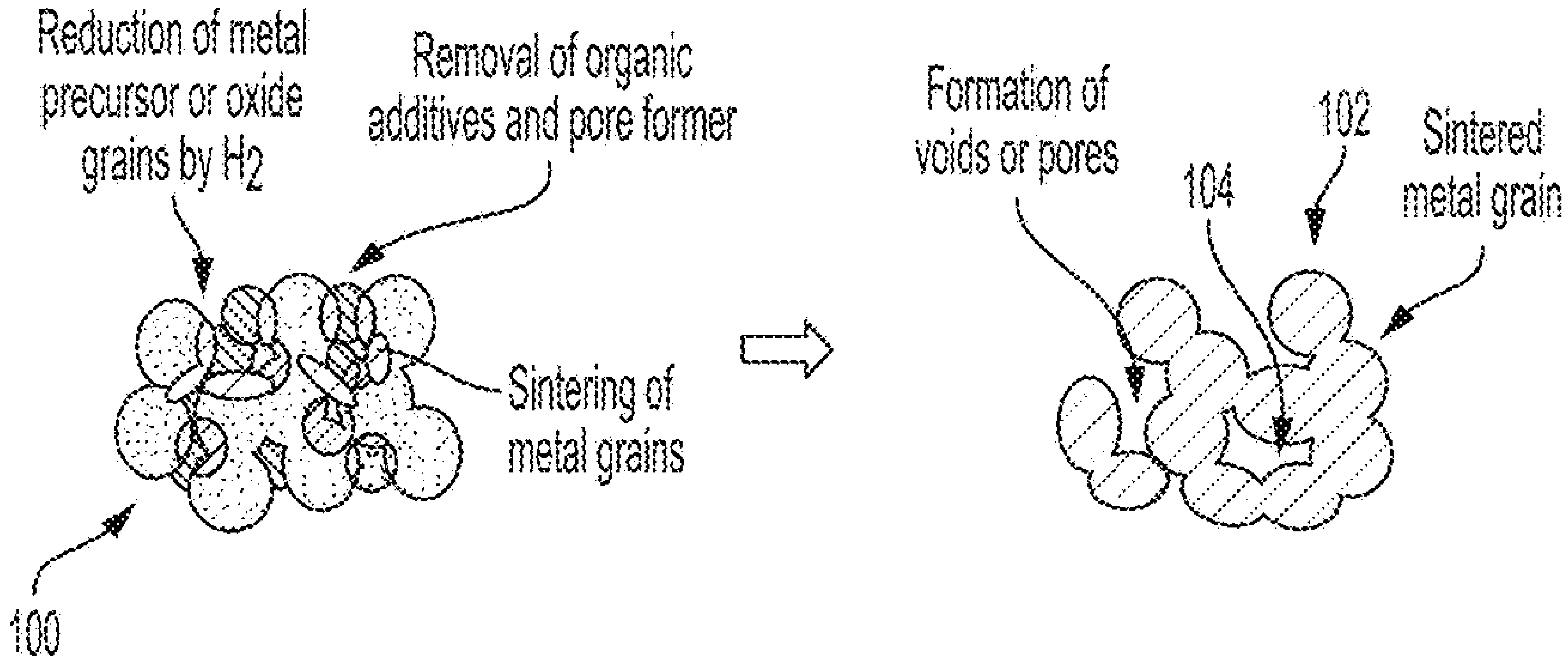
Reduction of metal precursor or oxide grains by H_2
Removal of organic additives and pore former
Sintering of metal grains
100
Formation of voids or pores
104
102
Sintered metal grain

FIG. 1

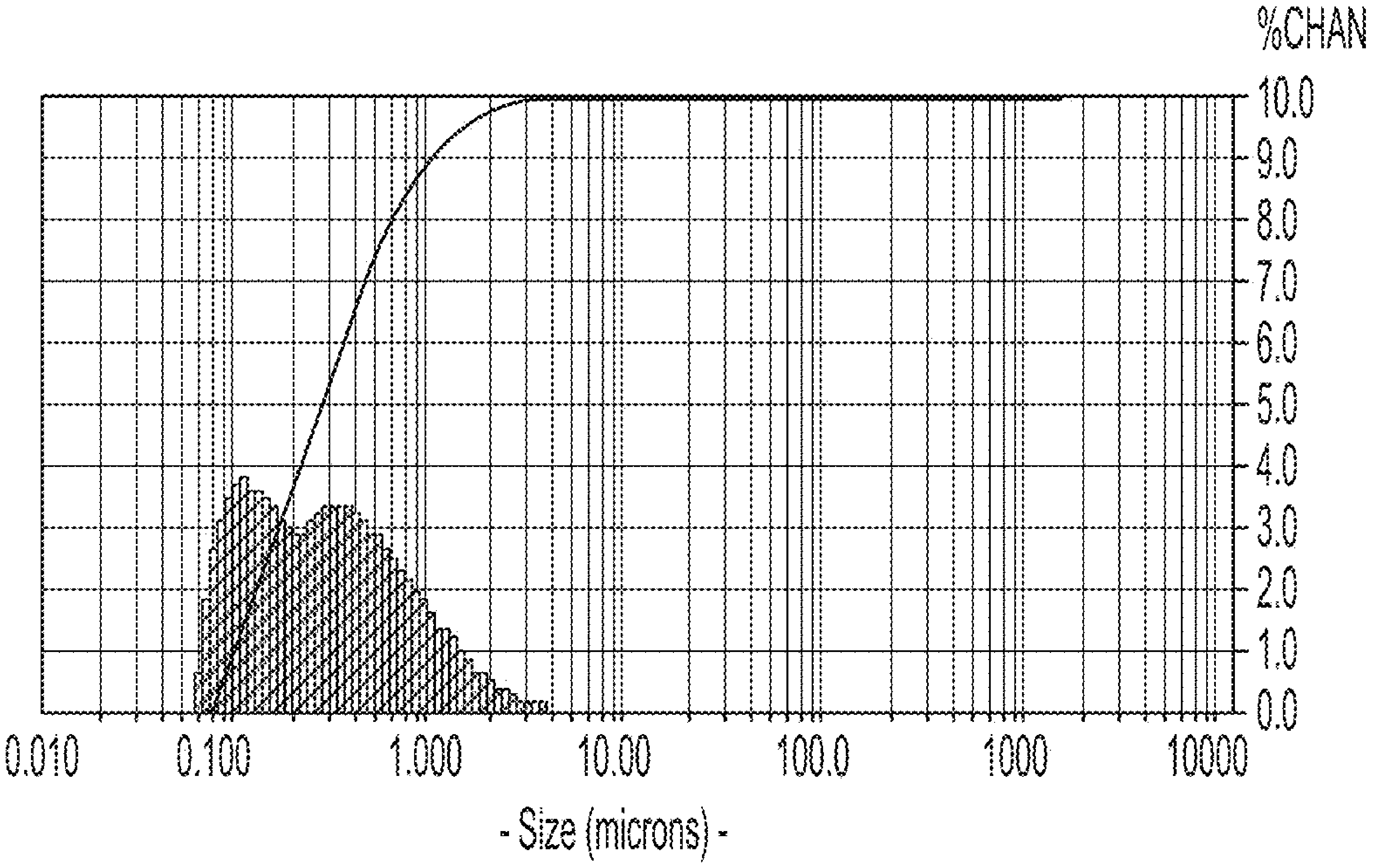
%CHAN
10.0
9.0
8.0
7.0
6.0
5.0
4.0
3.0
2.0
1.0
0.0
0.010
0.100
1.000
10.00
100.0
1000
10000
- Size (microns) -

FIG. 2

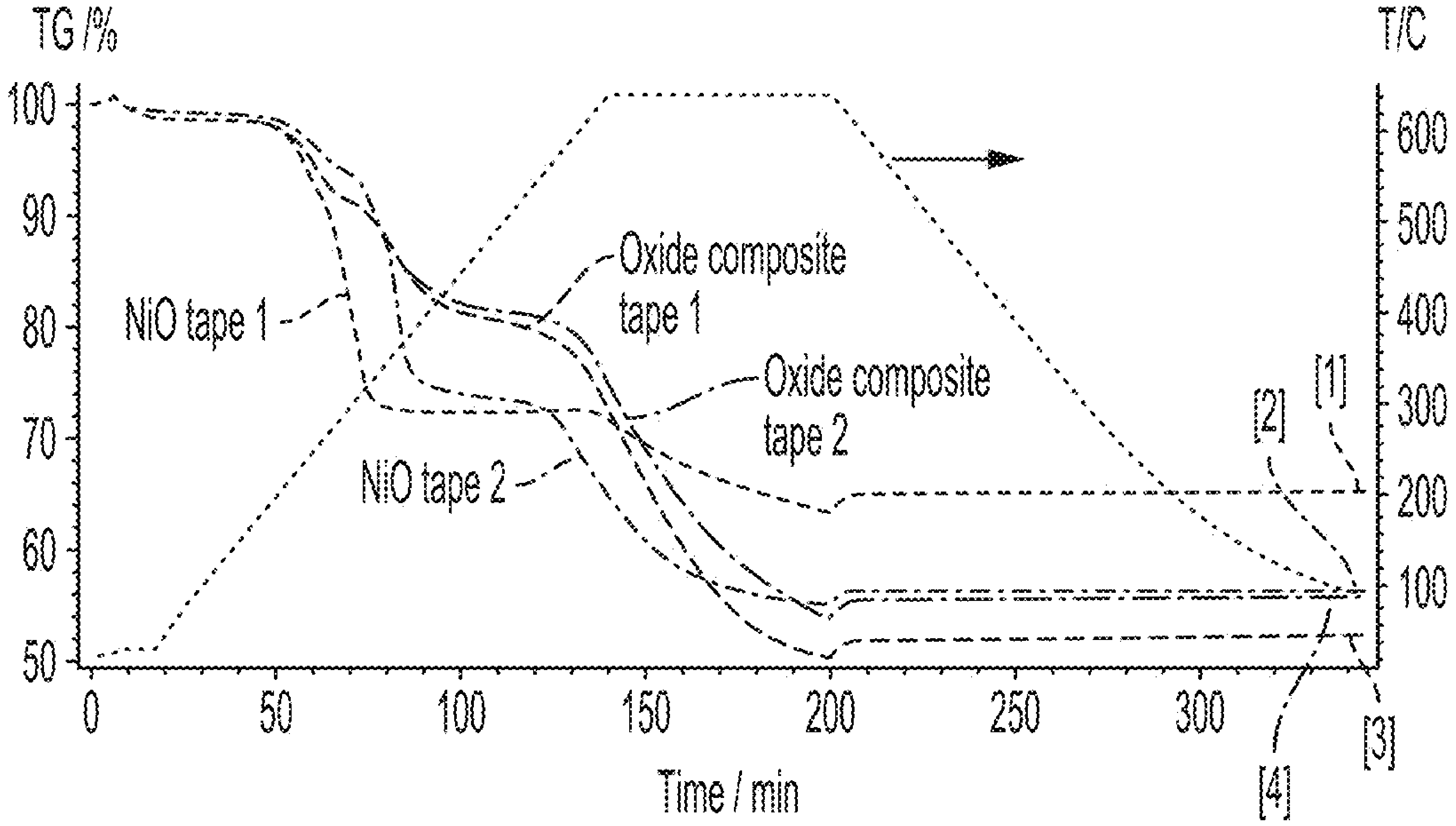
TG /%
T/C
100
90
80
70
60
50
600
500
400
300
200
100
0
50
100
150
200
250
300
Time / min
NiO tape 1
NiO tape 2
Oxide composite tape 1
Oxide composite tape 2
[1]
[2]
[3]
[4]

FIG. 3

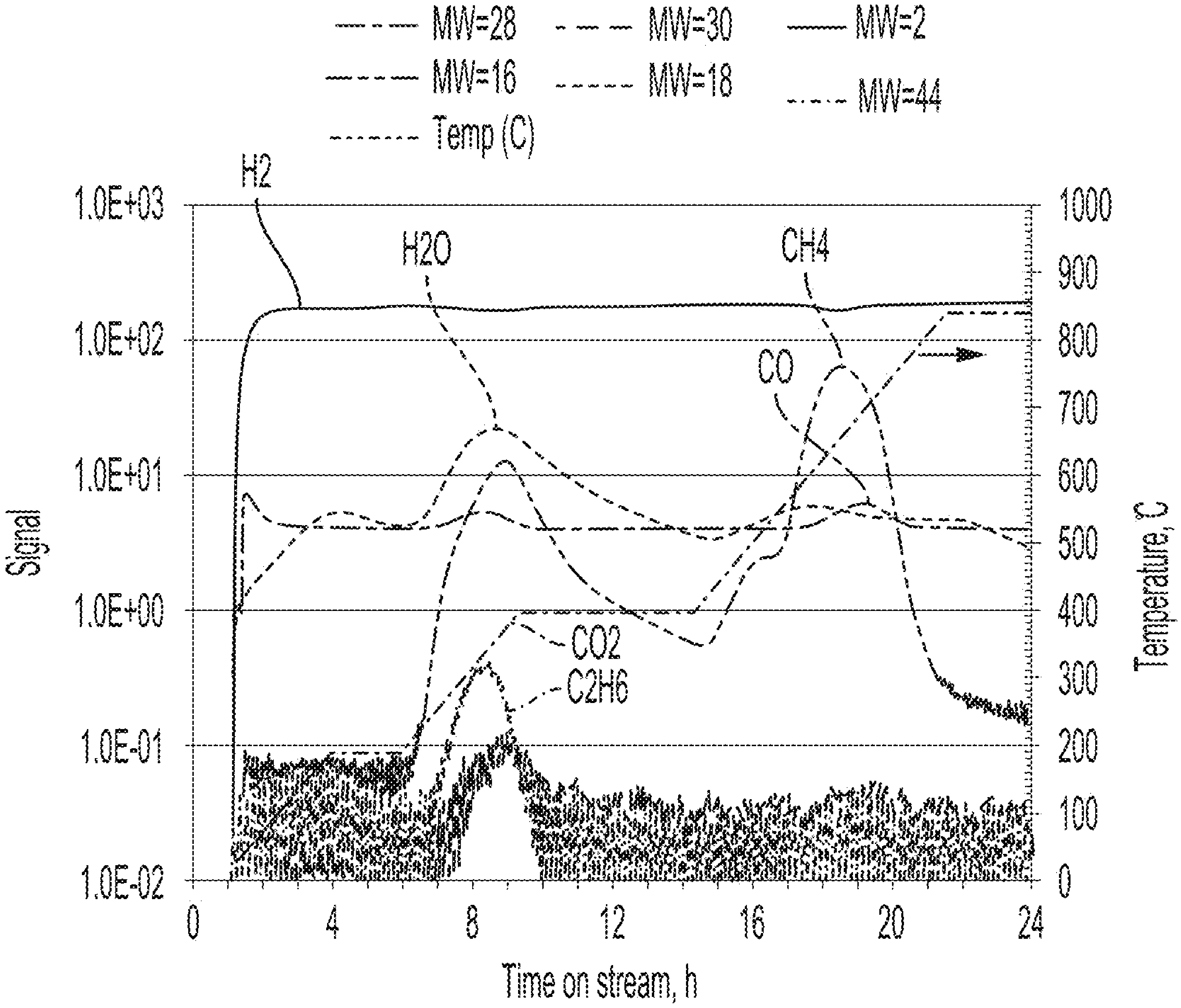
MW=28
MW=30
MW=2
MW=16
MW=18
MW=44
Temp (C)
H2
H2O
CH4
CO
CO2
C2H6
1.0E+03
1.0E+02
1.0E+01
1.0E+00
1.0E-01
1.0E-02
Signal
1000
900
800
700
600
500
400
300
200
100
0
Temperature, C
0
4
8
12
16
20
24
Time on stream, h

FIG. 4

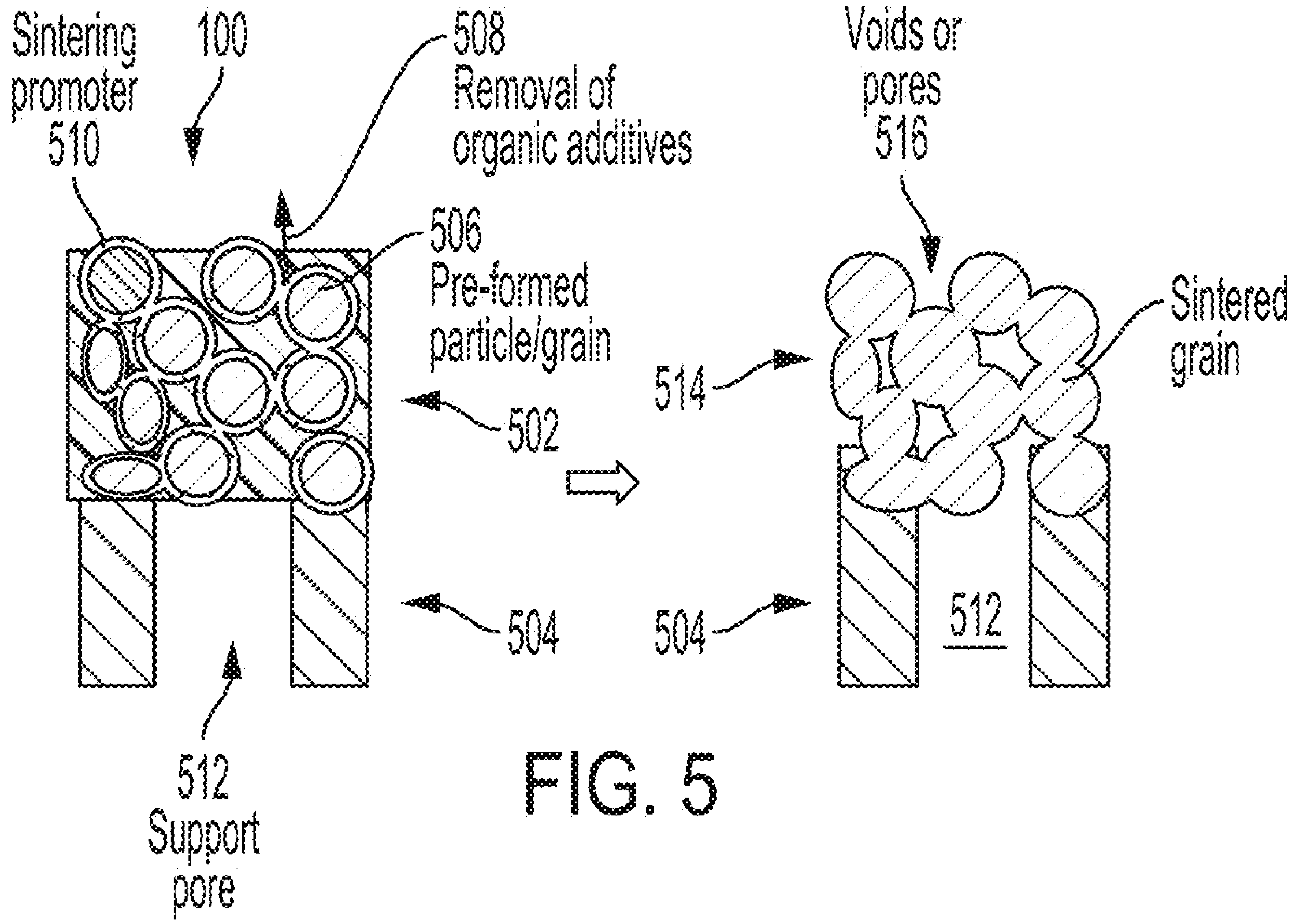

FIG. 5

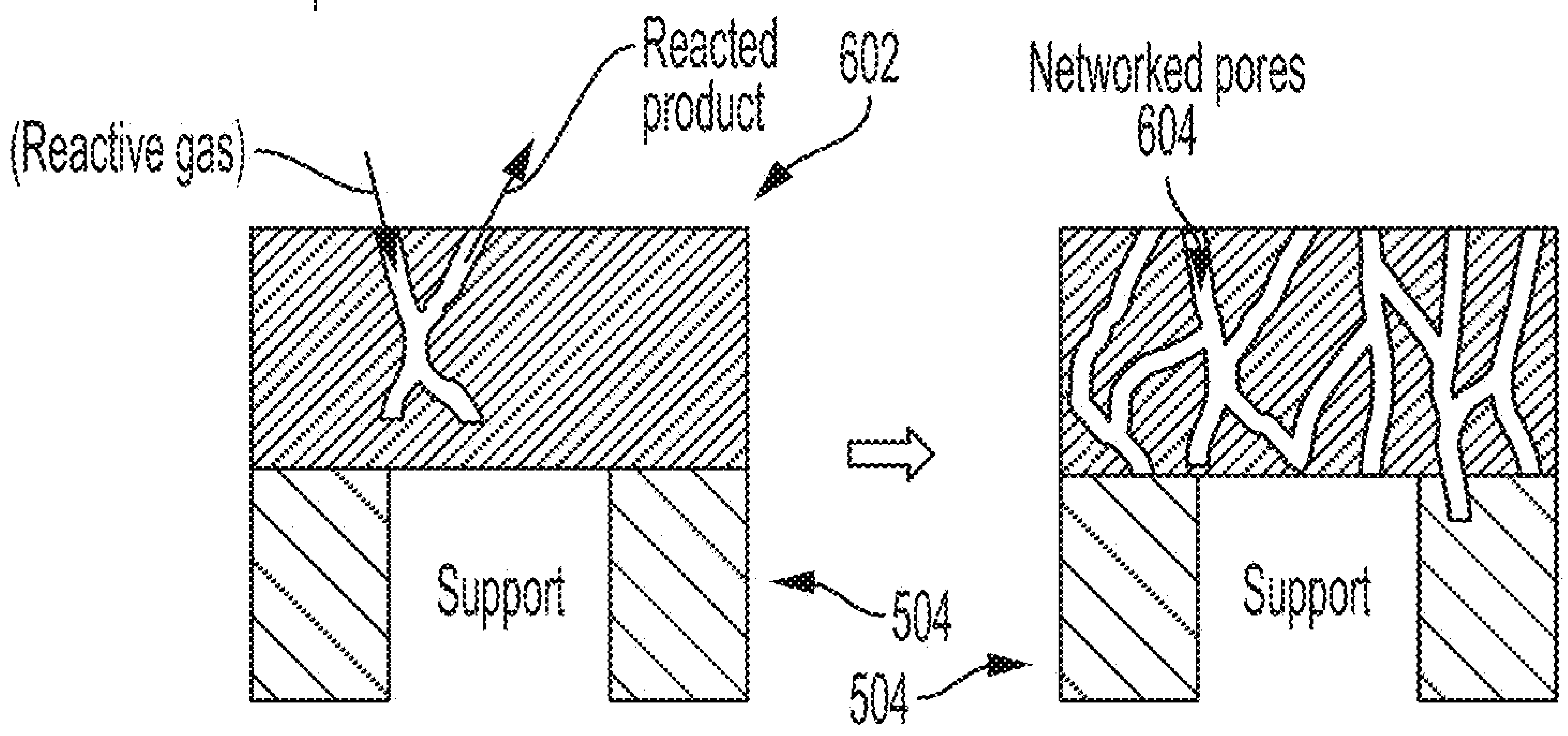

FIG. 6A

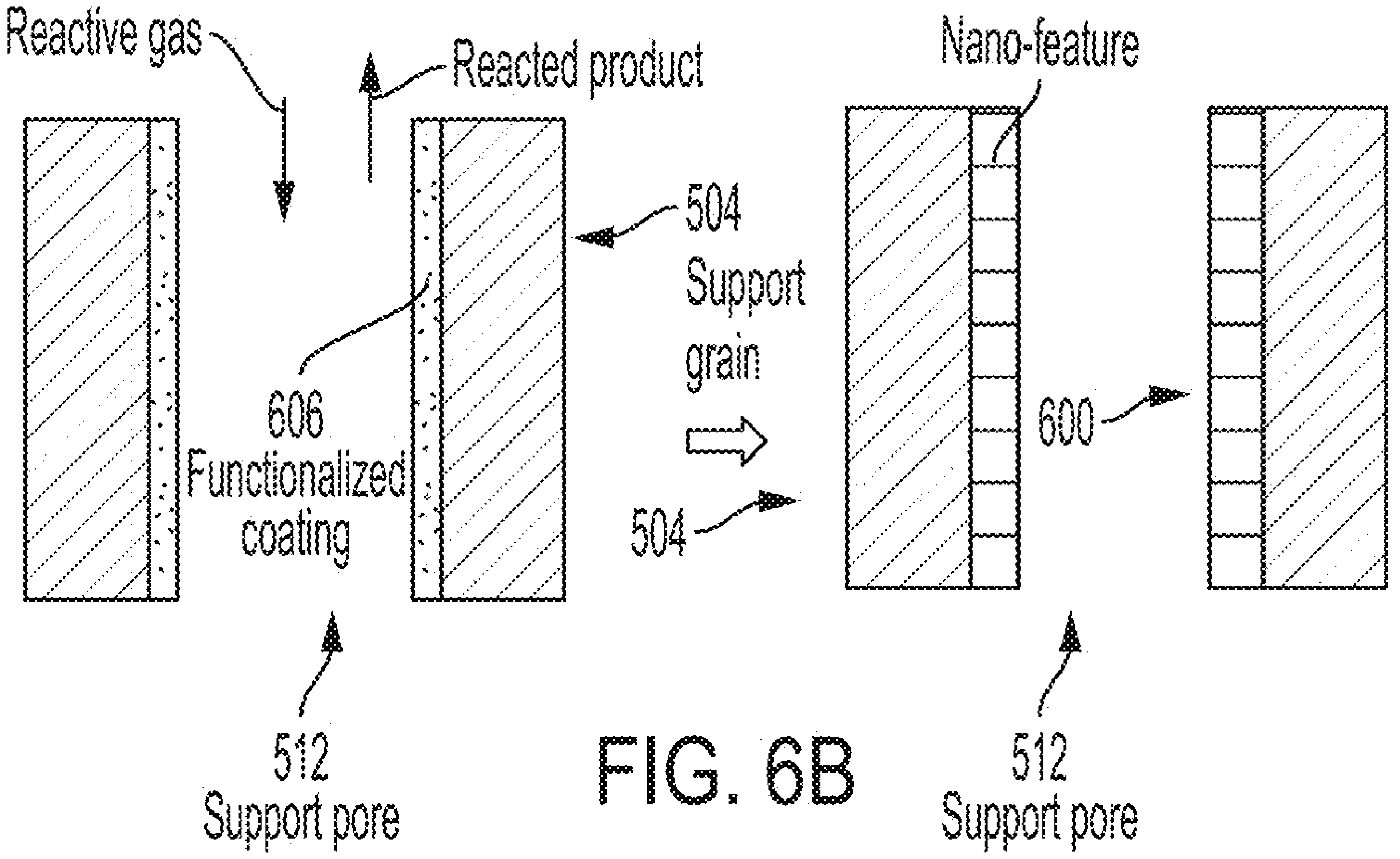

FIG. 6B

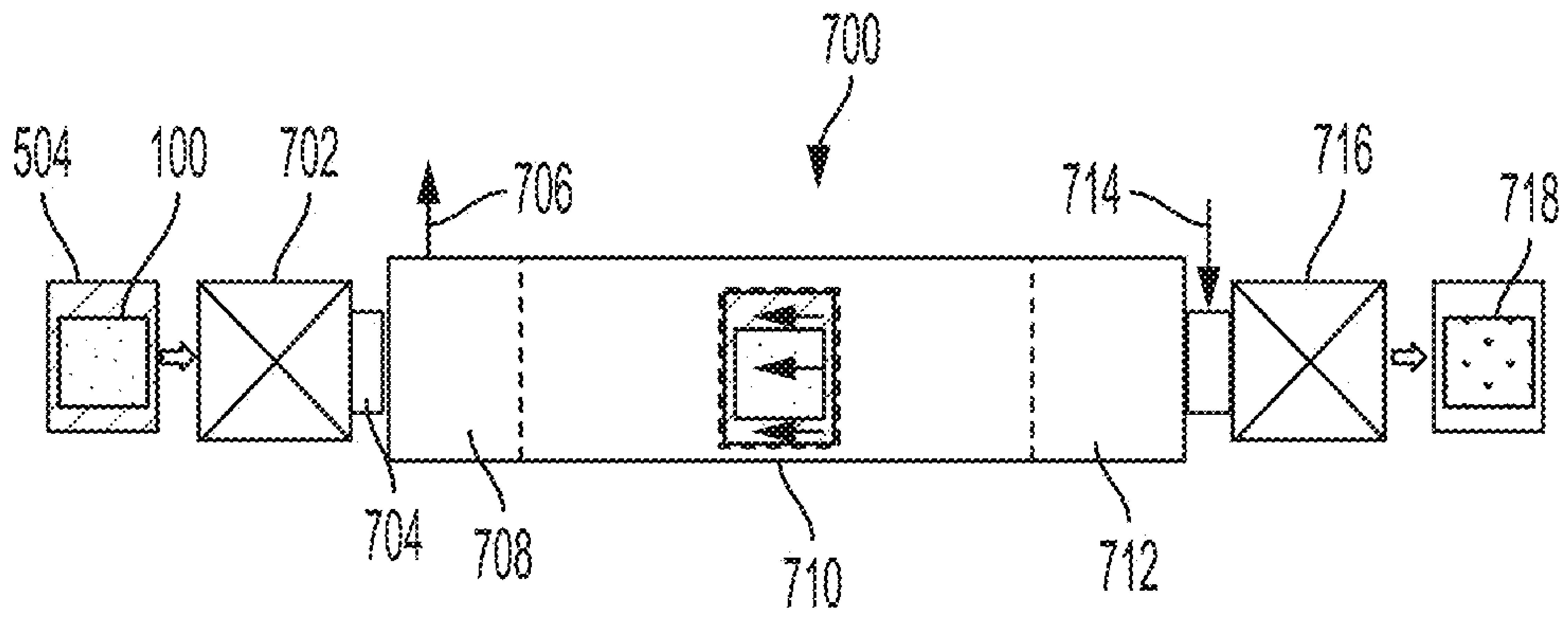
700
504
100
702
706
714
716
718
704
708
710
712

FIG. 7

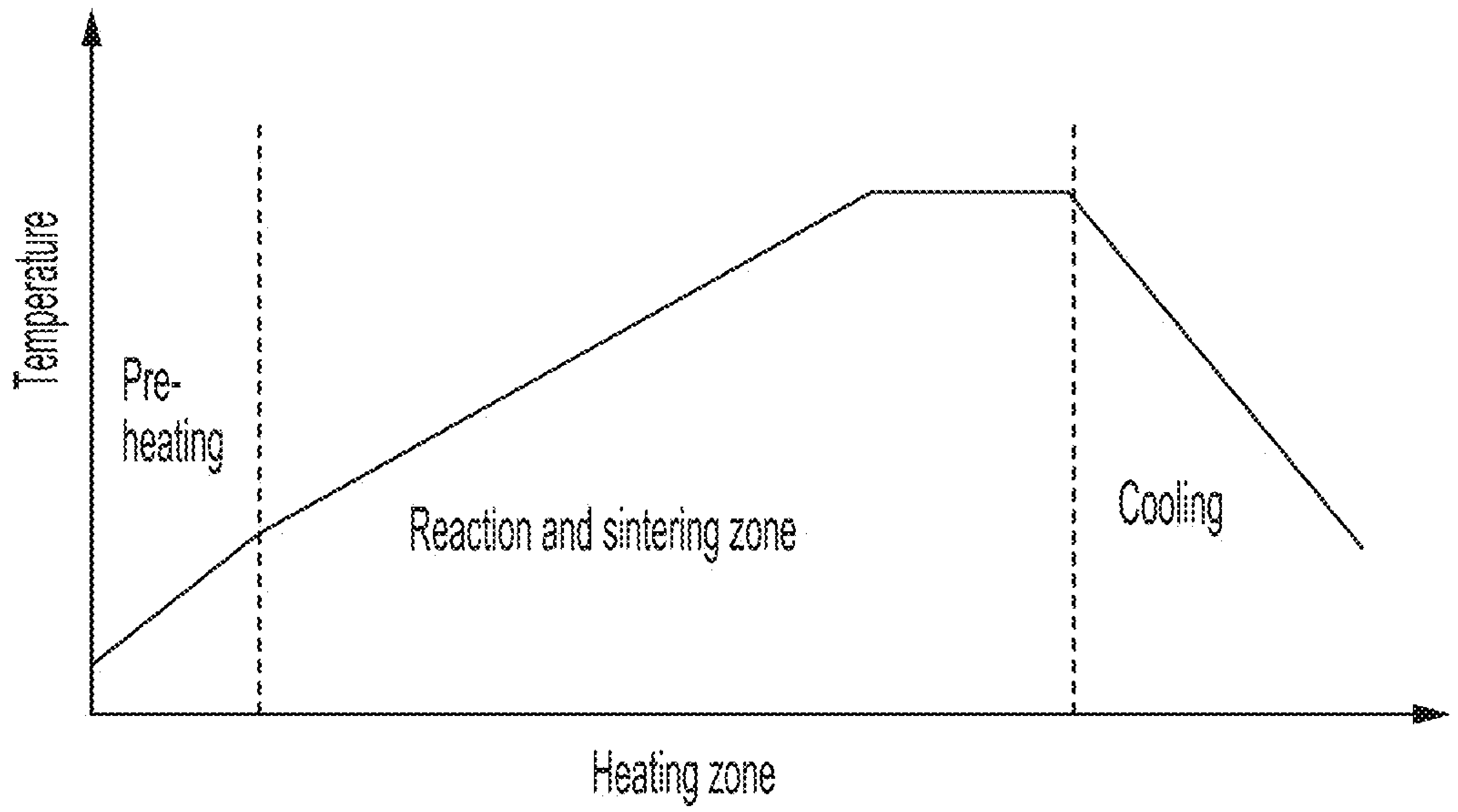
Temperature
Pre-
heating
Reaction and sintering zone
Cooling
Heating zone

FIG. 8

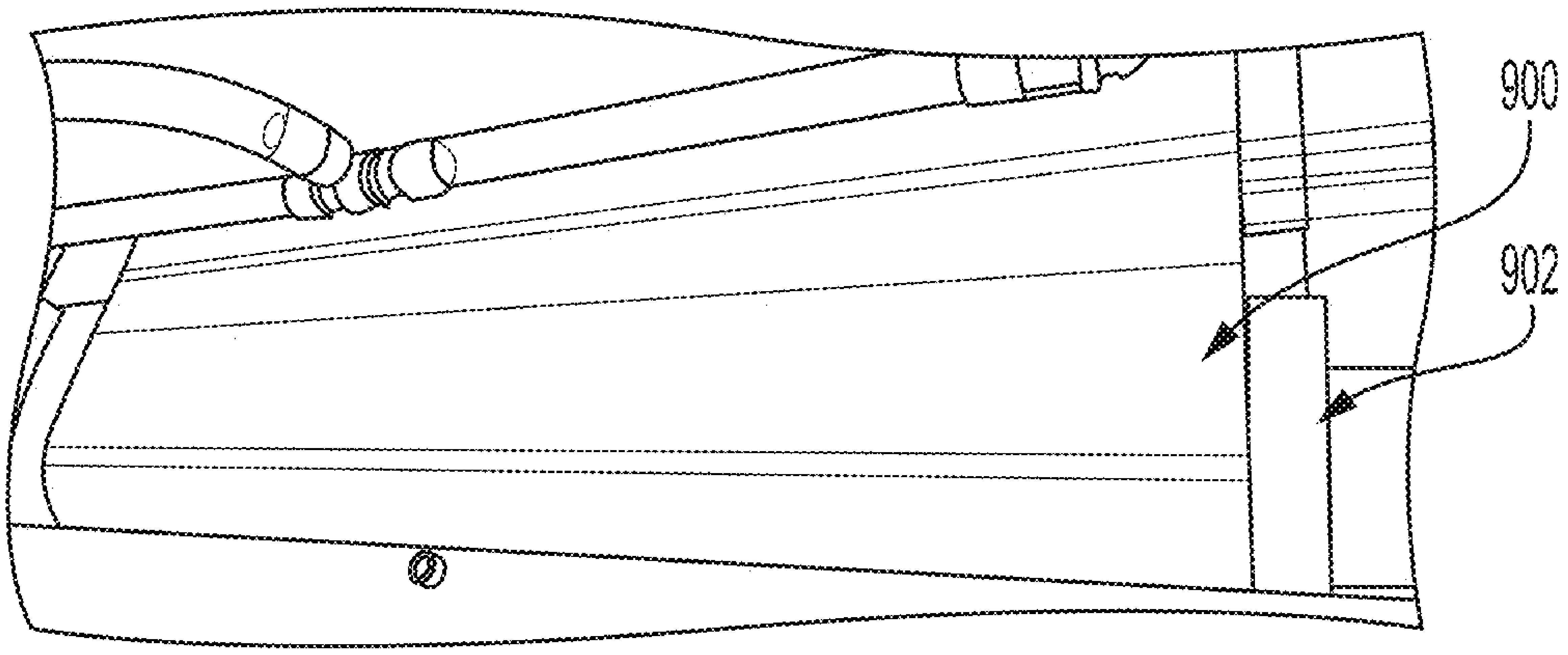

FIG. 9A

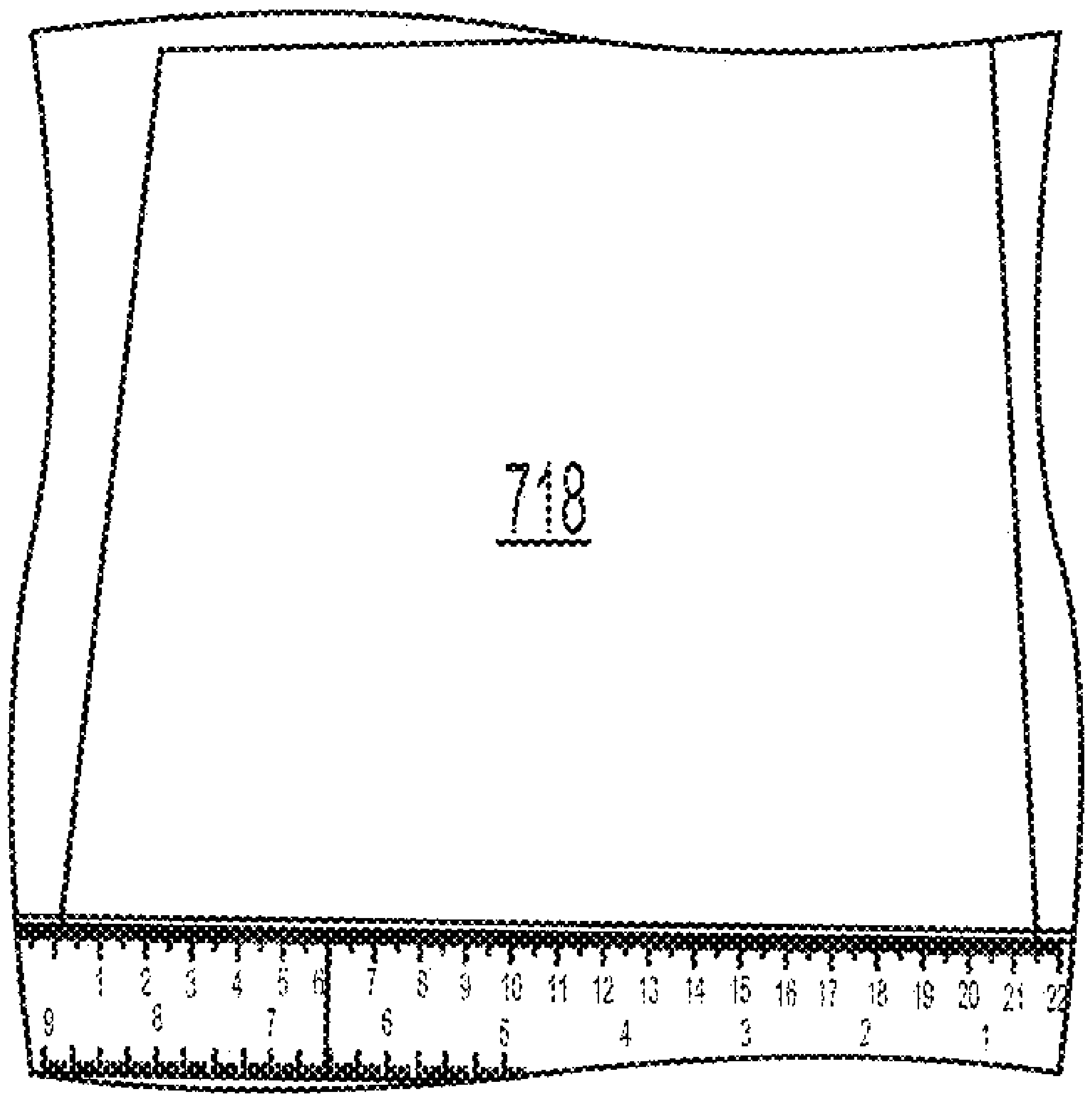

FIG. 9B

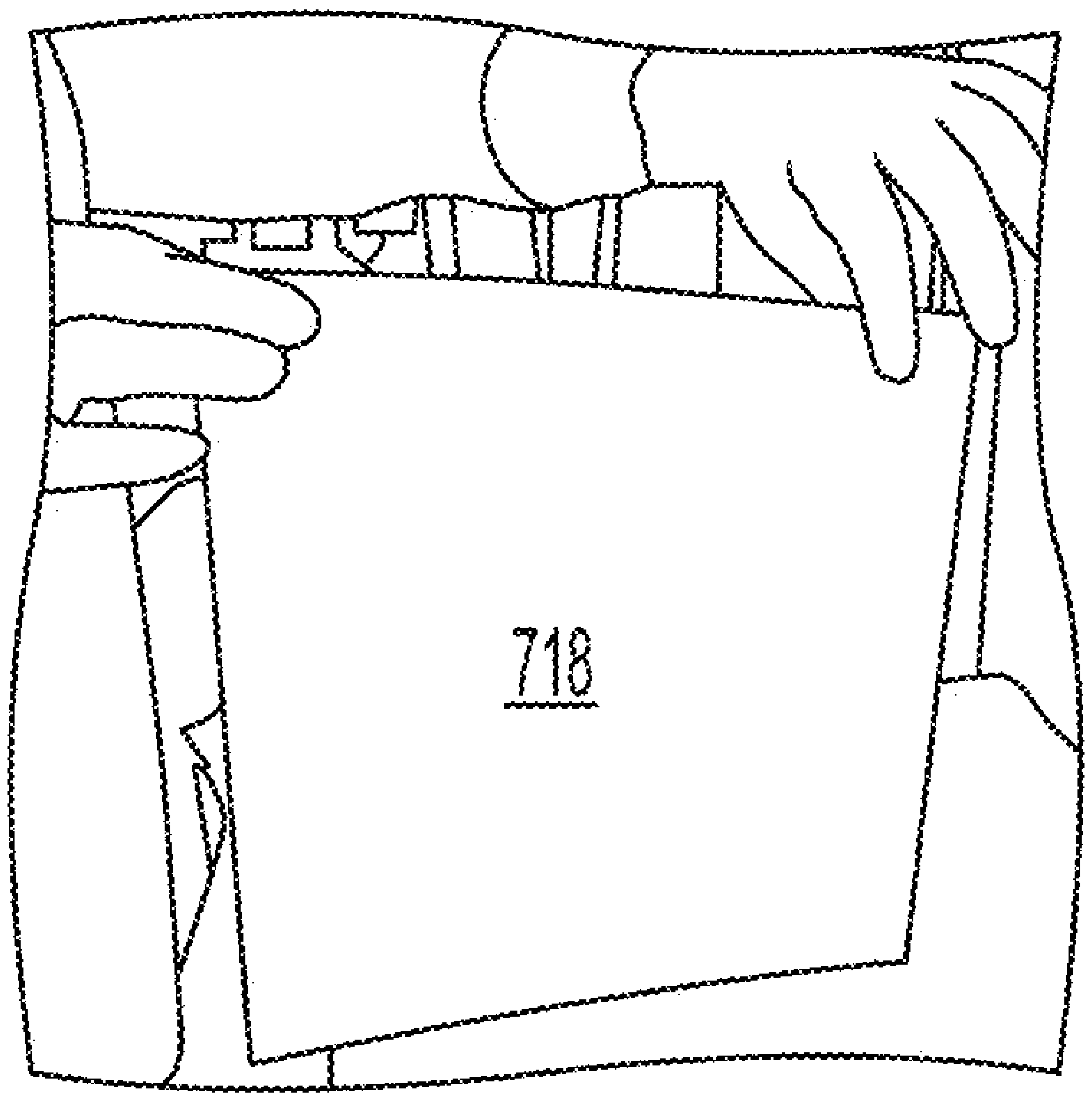

FIG. 9C

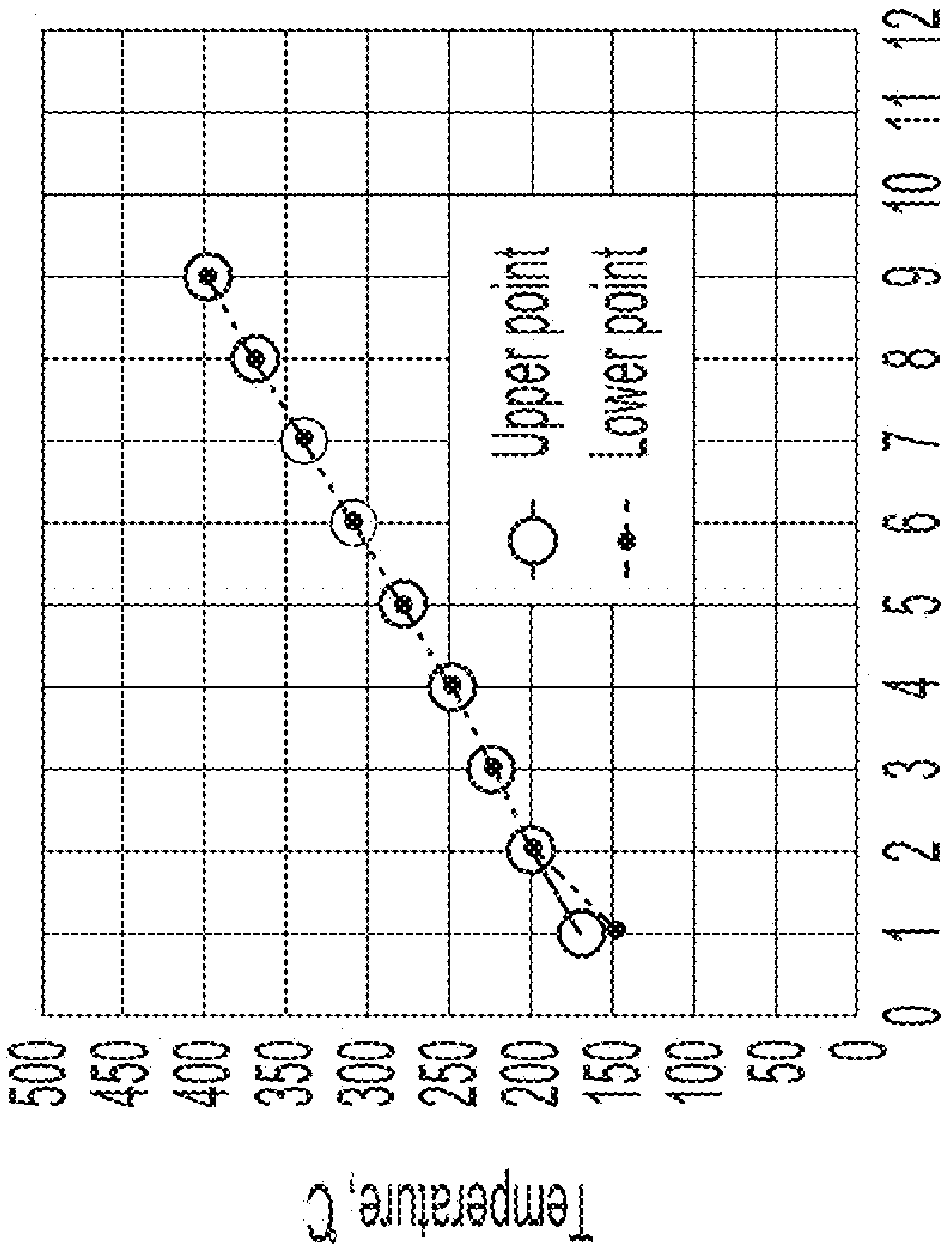

FIG. 10A

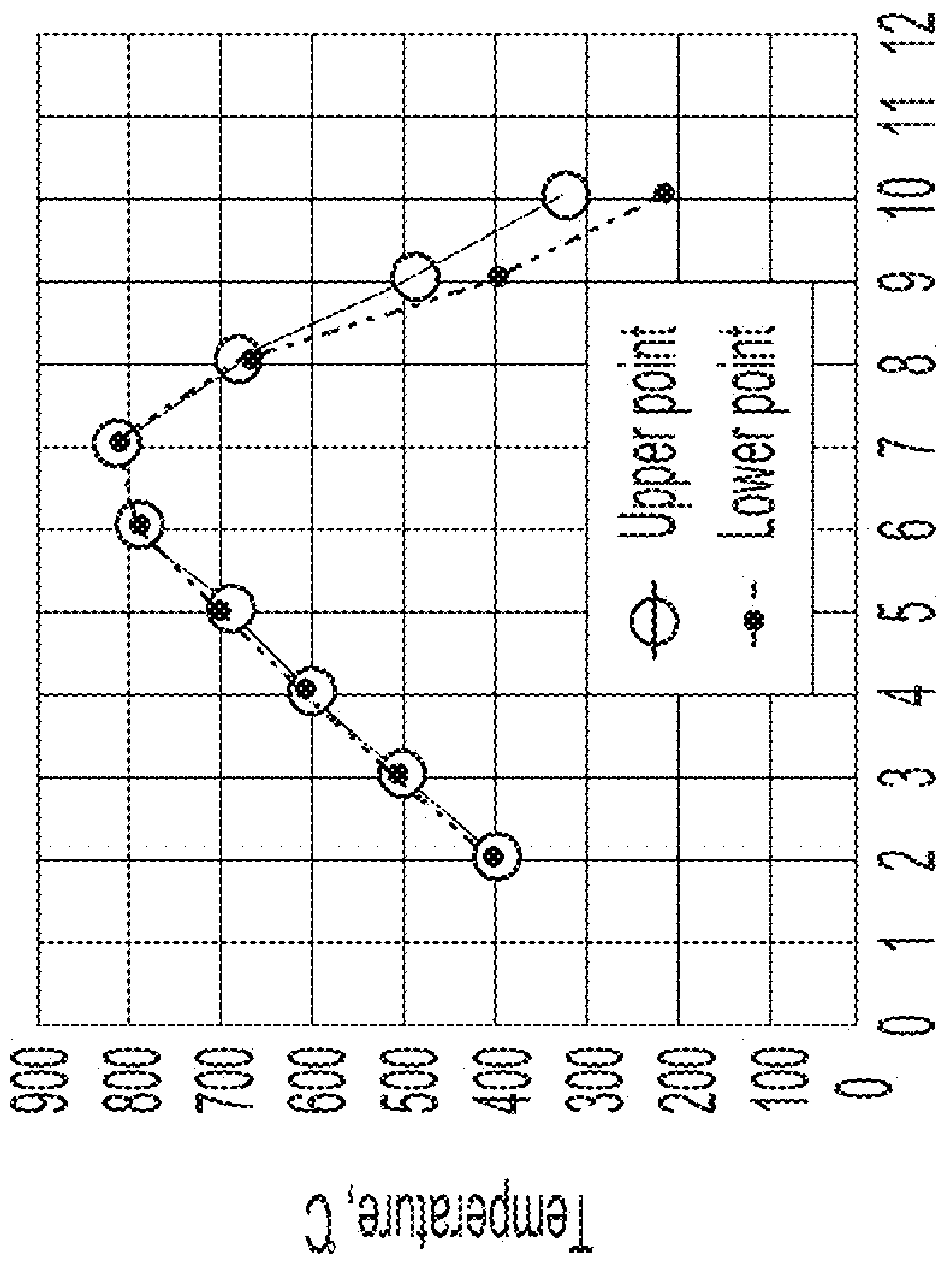

FIG. 10B

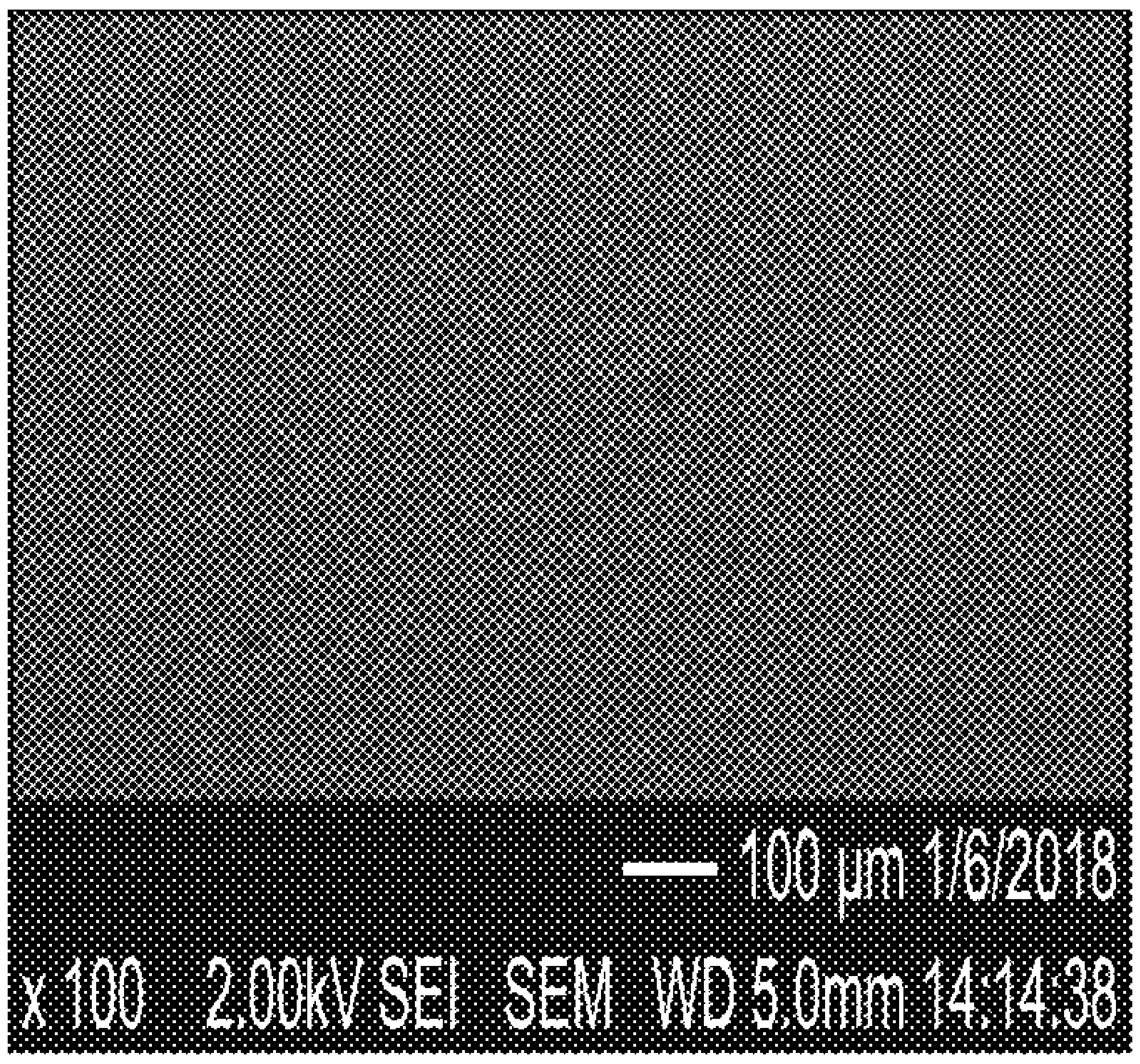

FIG. 11A

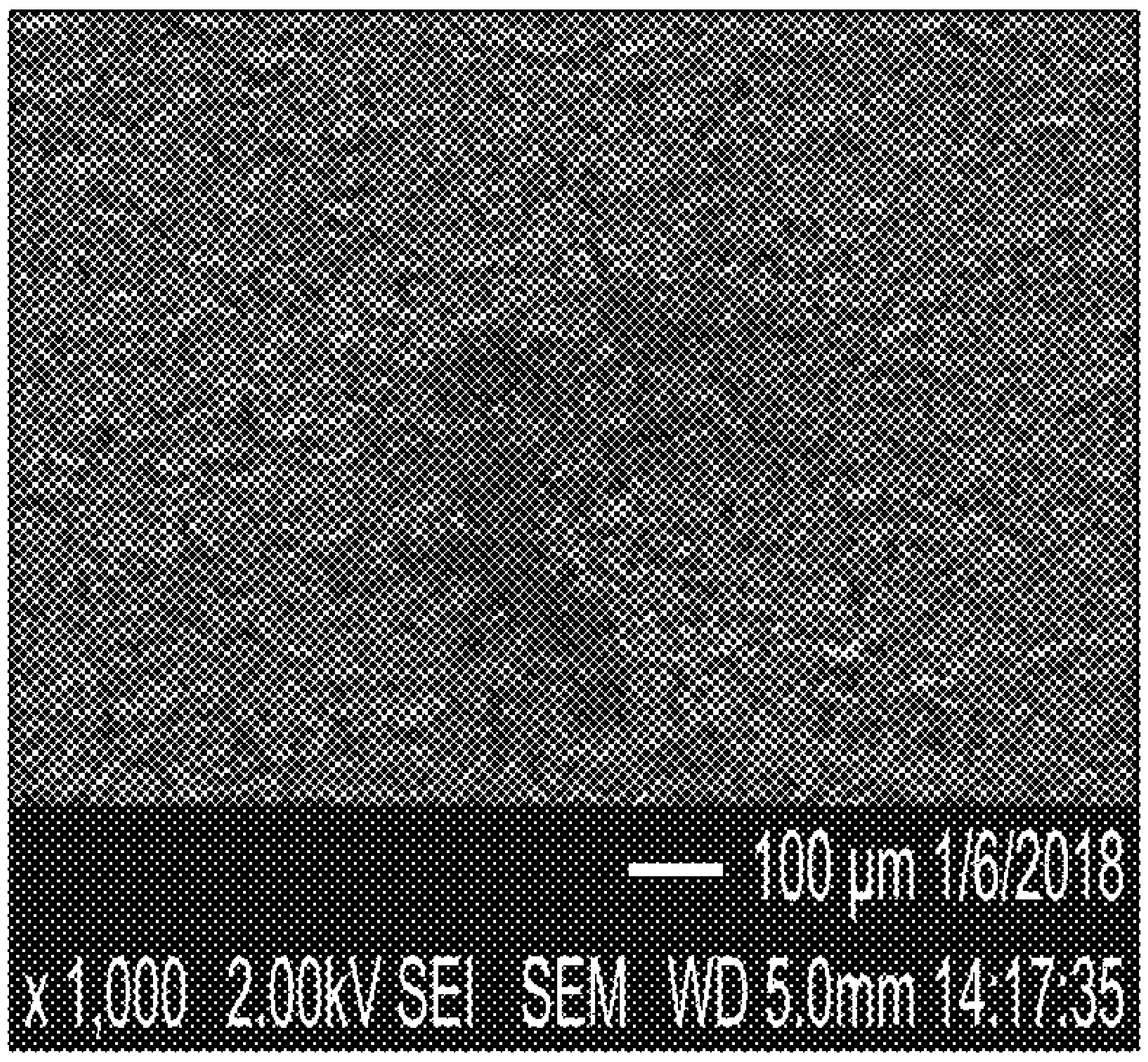

FIG. 11B

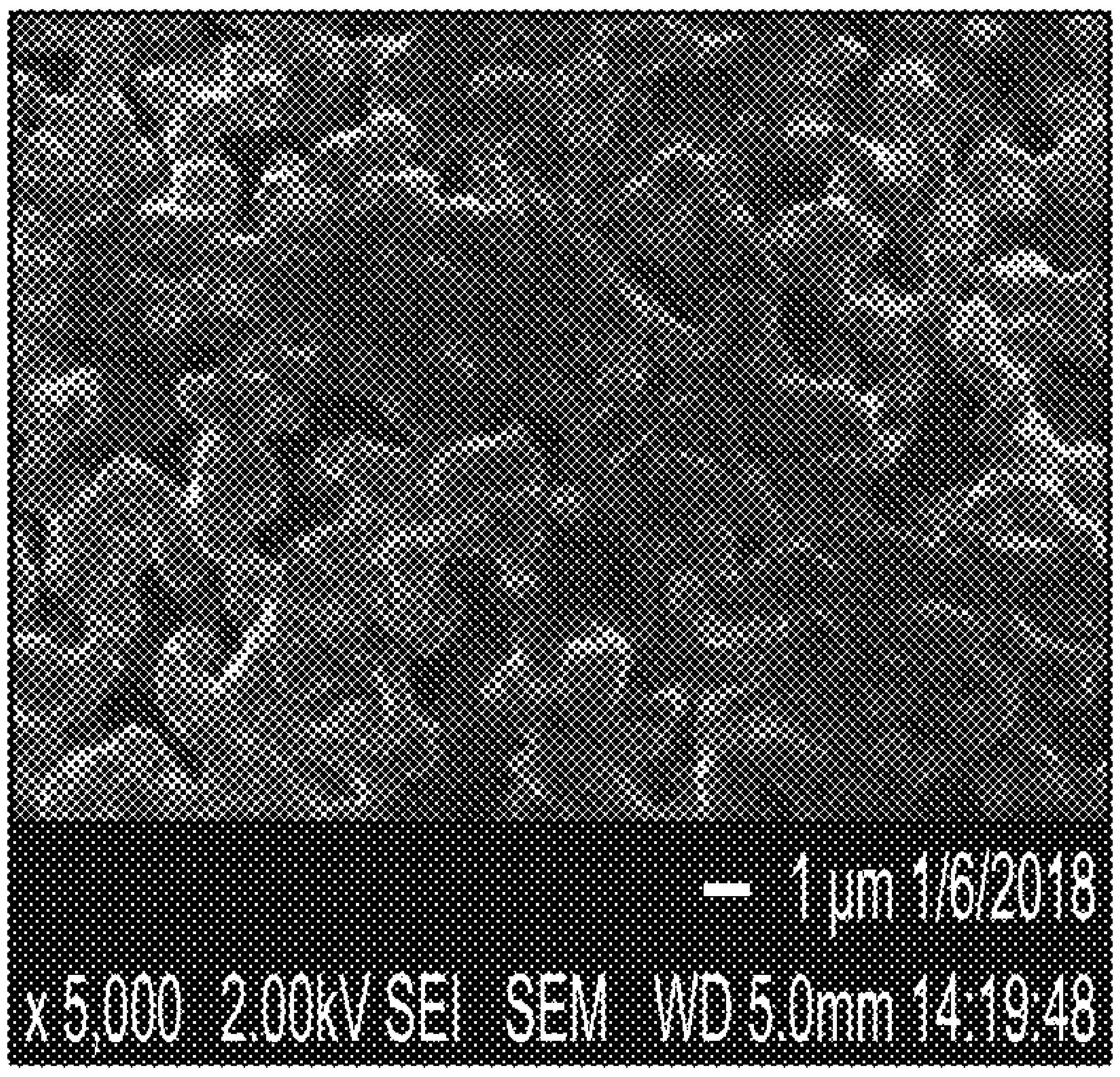

FIG. 11C

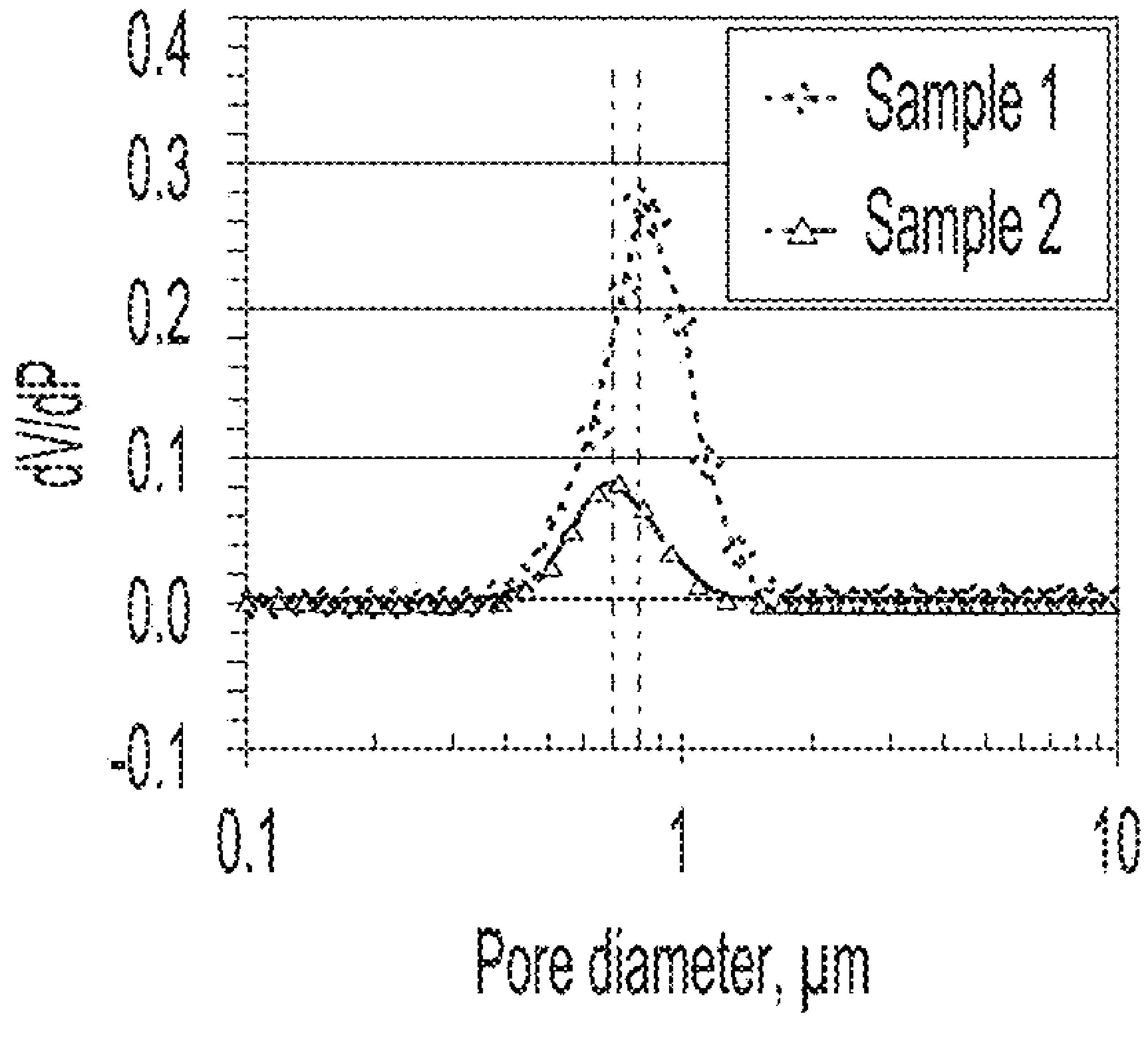

FIG. 11D

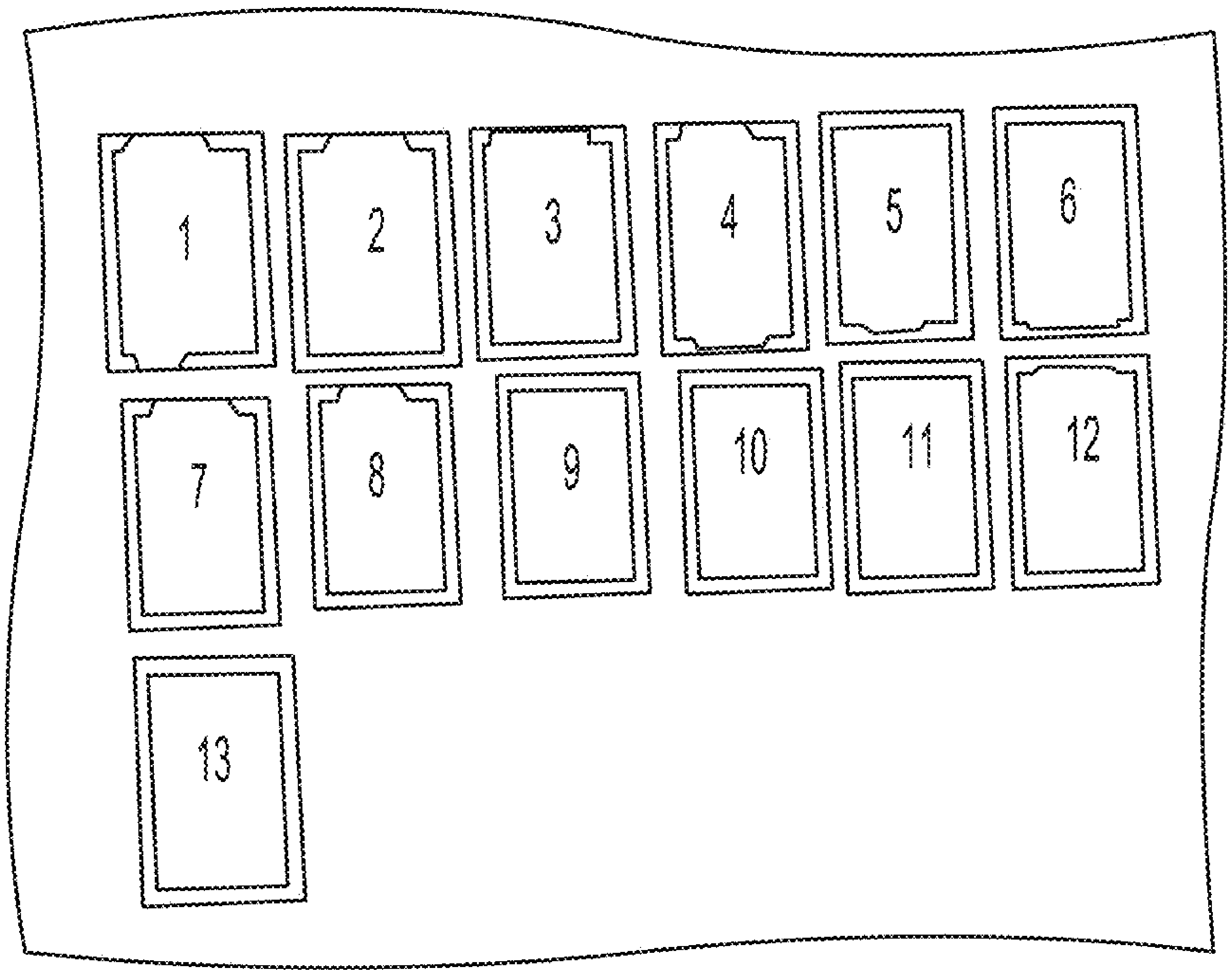

FIG. 12A

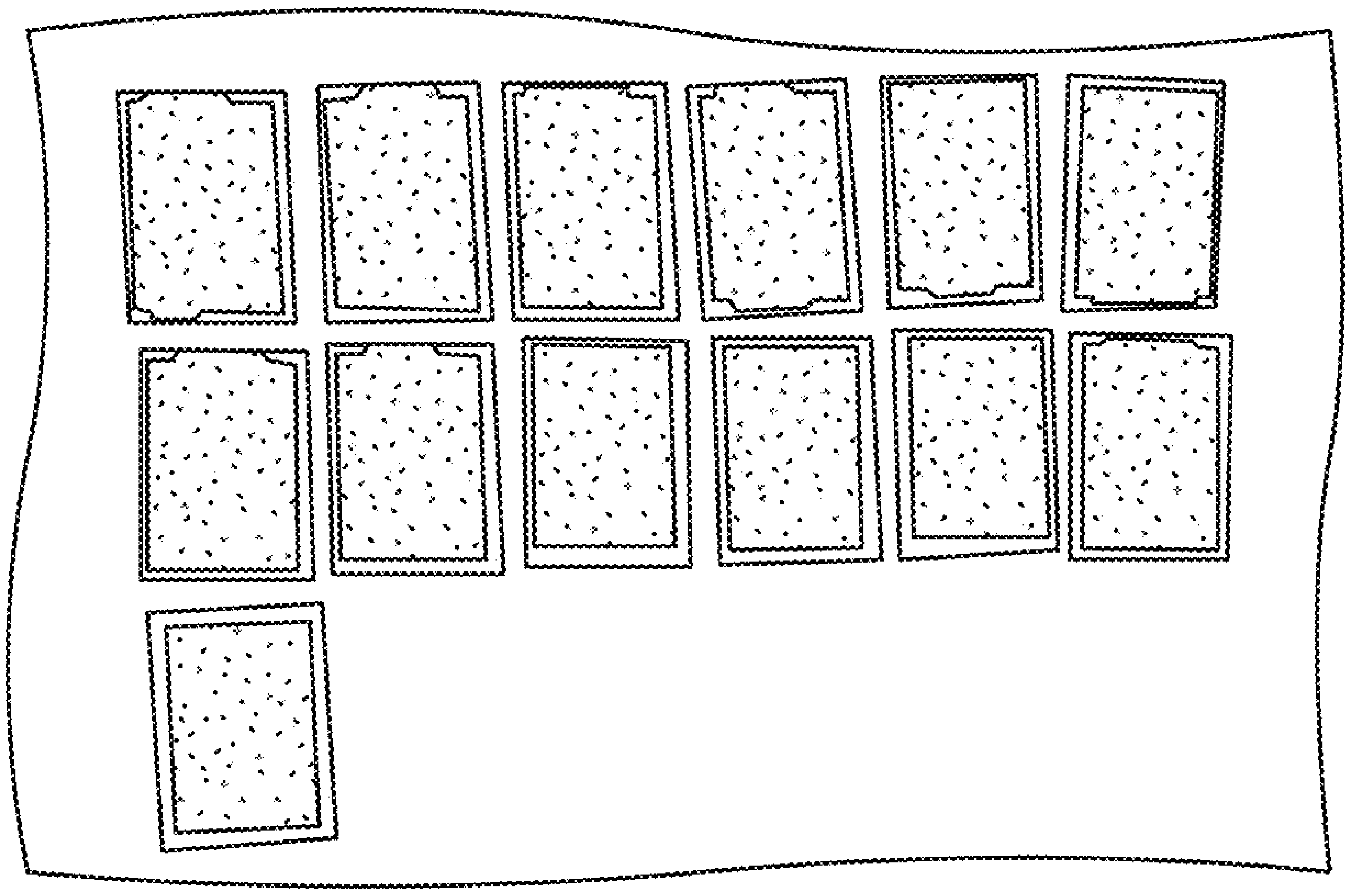

FIG. 12B

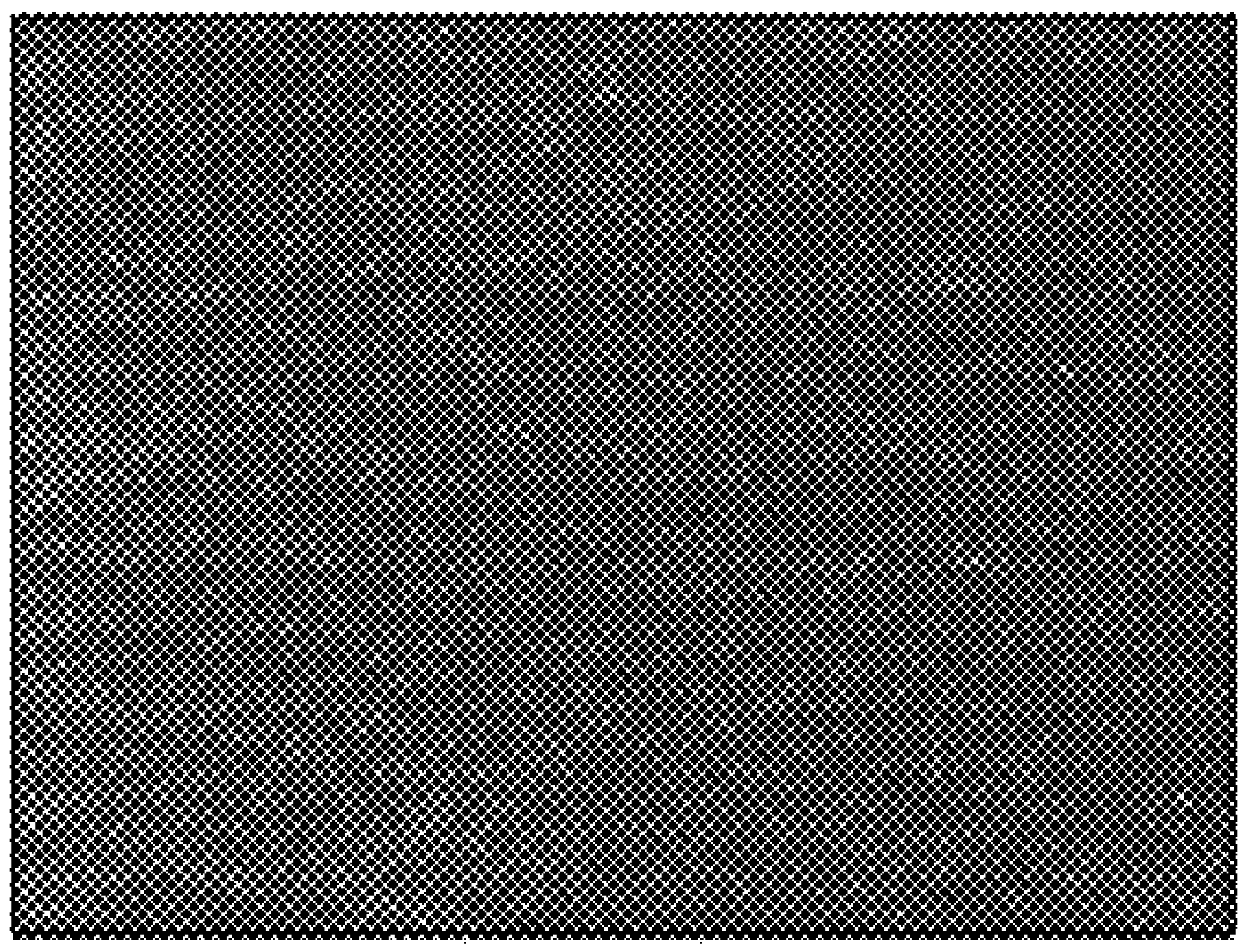

FIG. 13A

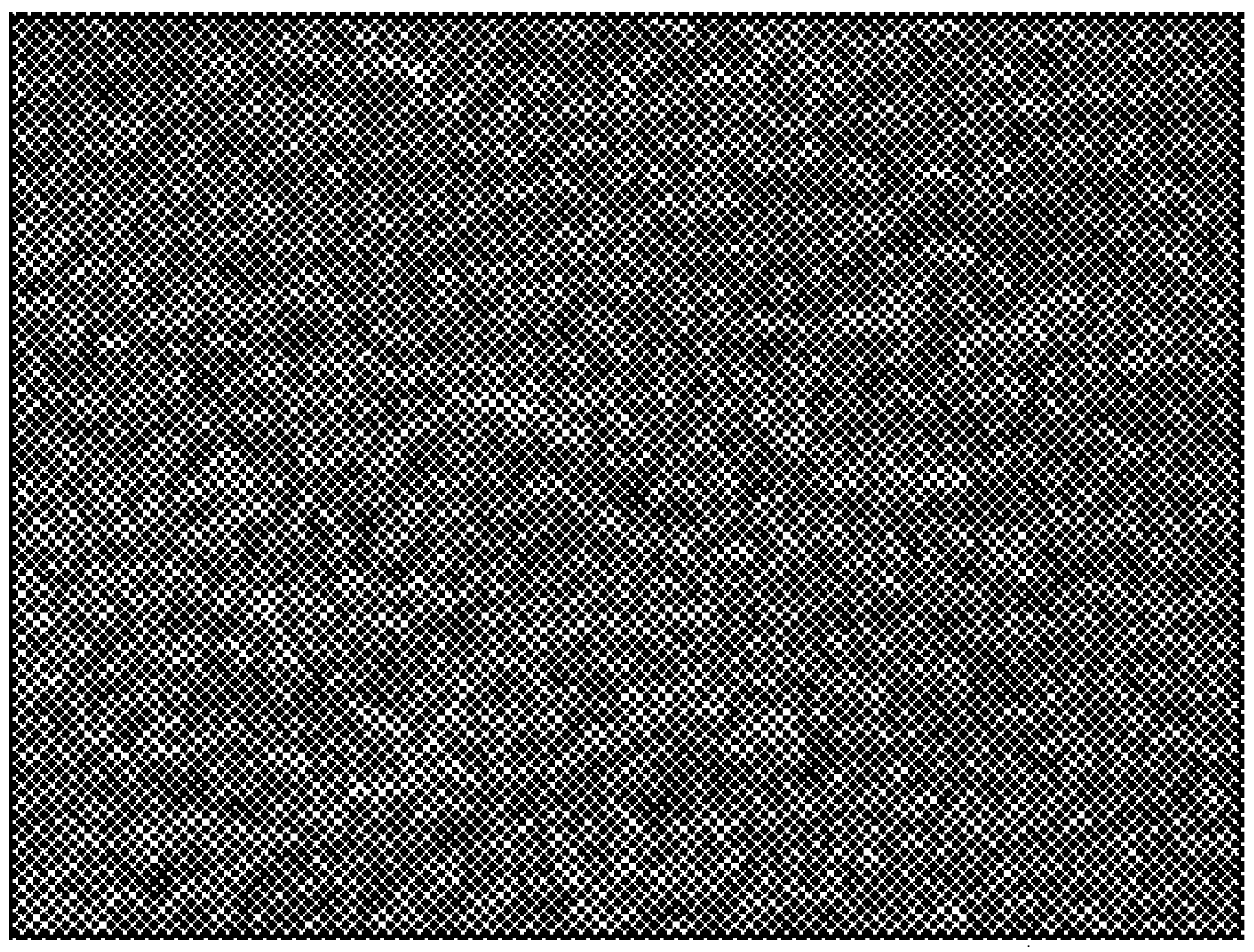

FIG. 13B

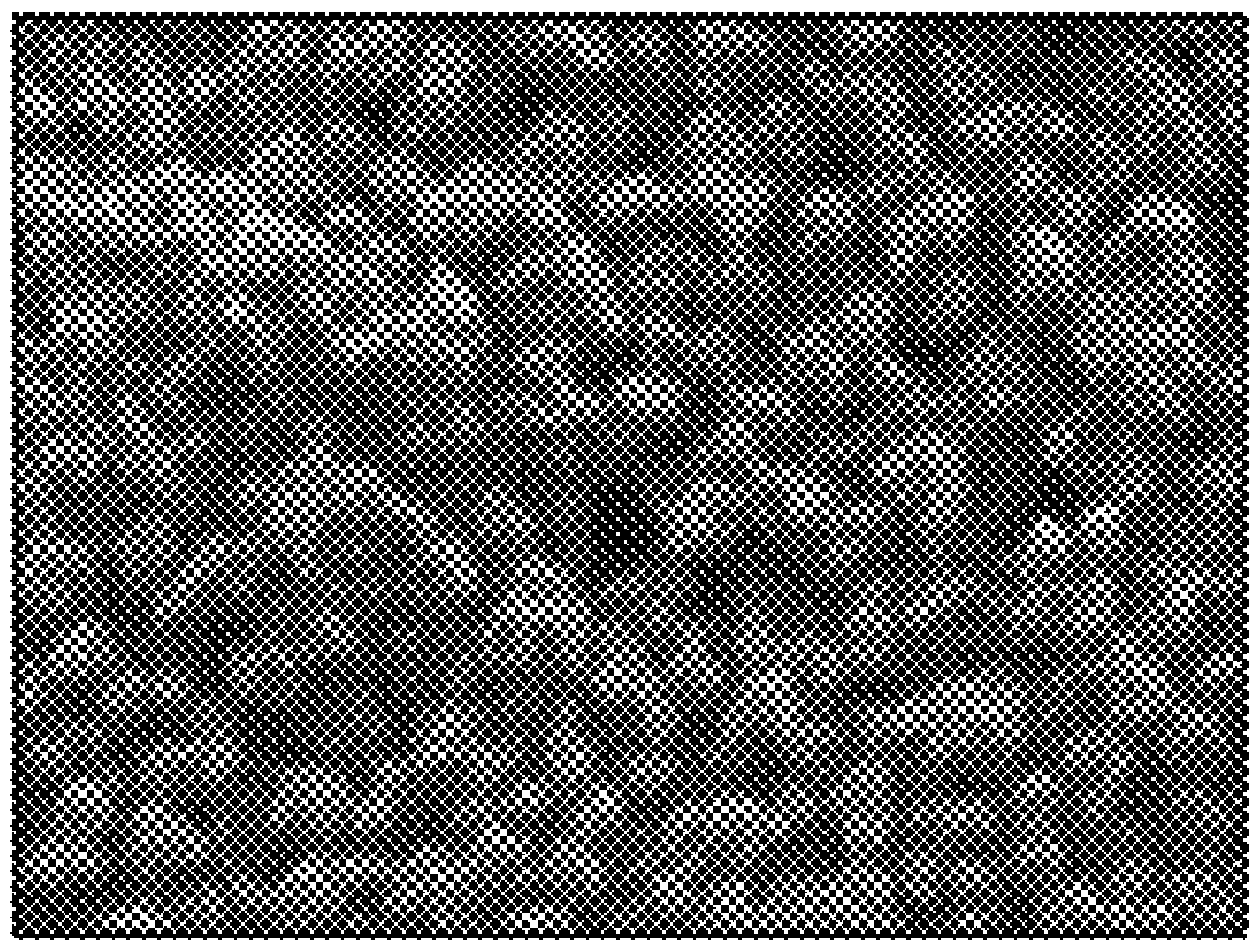

FIG. 13C

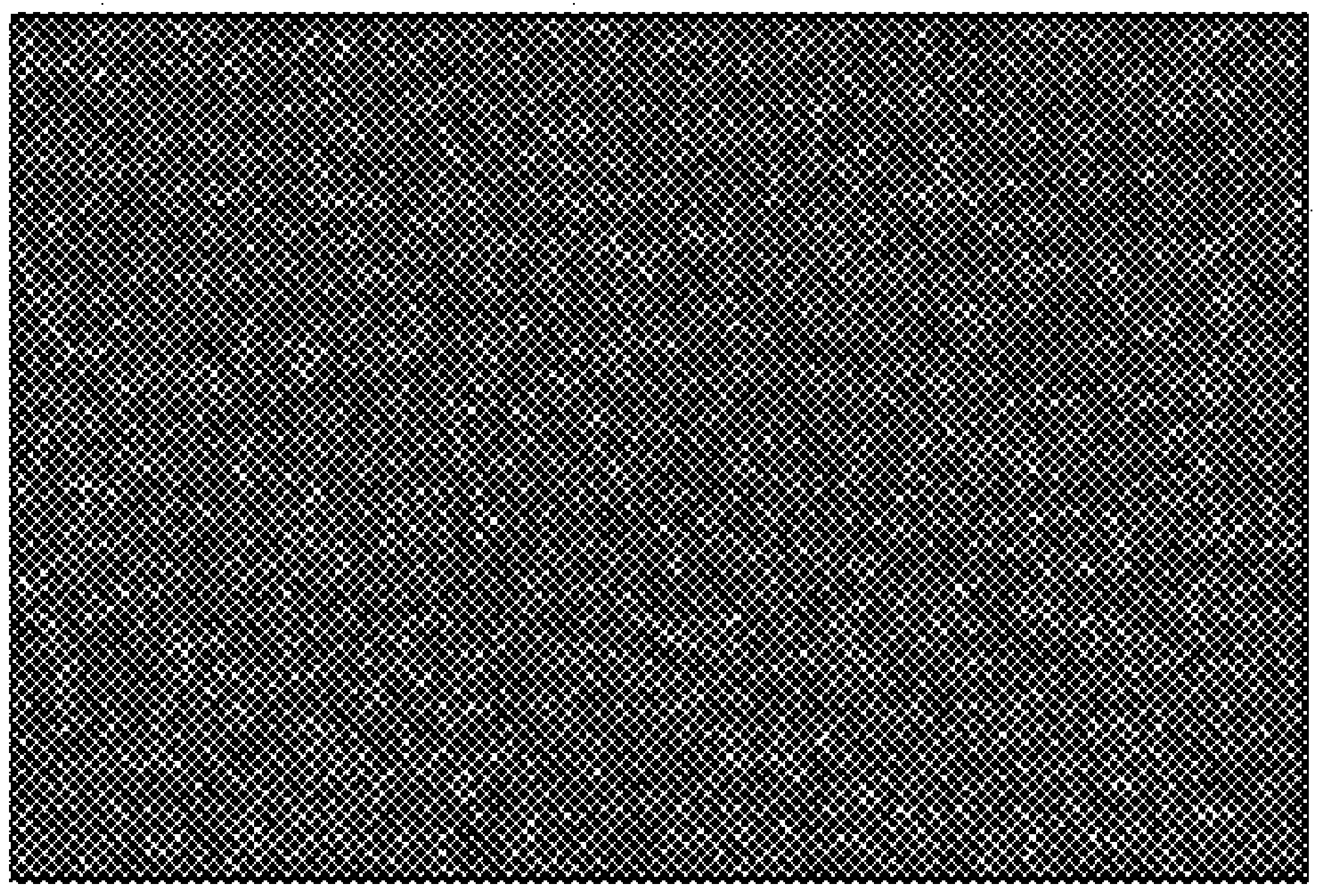

FIG. 13D

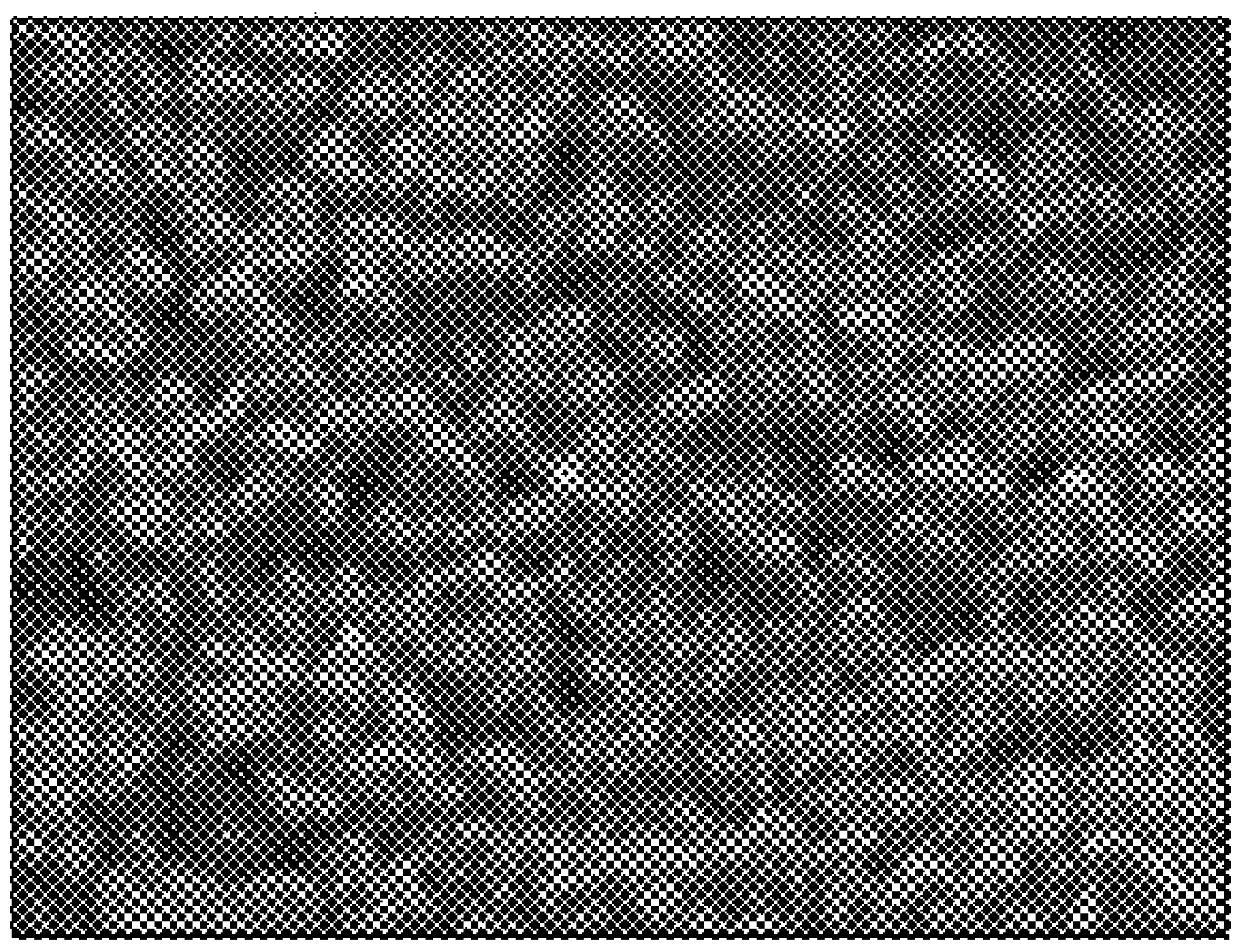

FIG. 14A

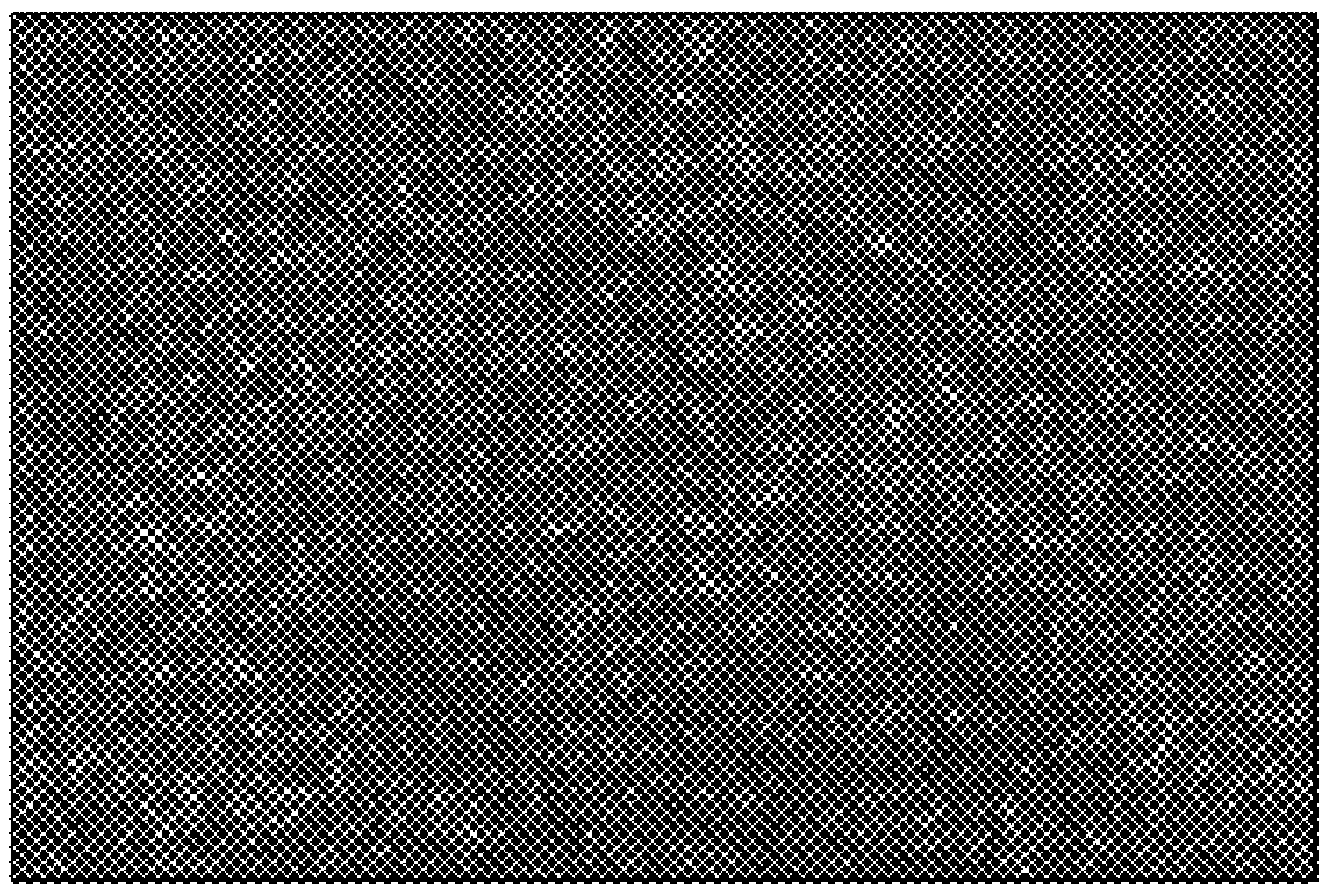

FIG. 14B

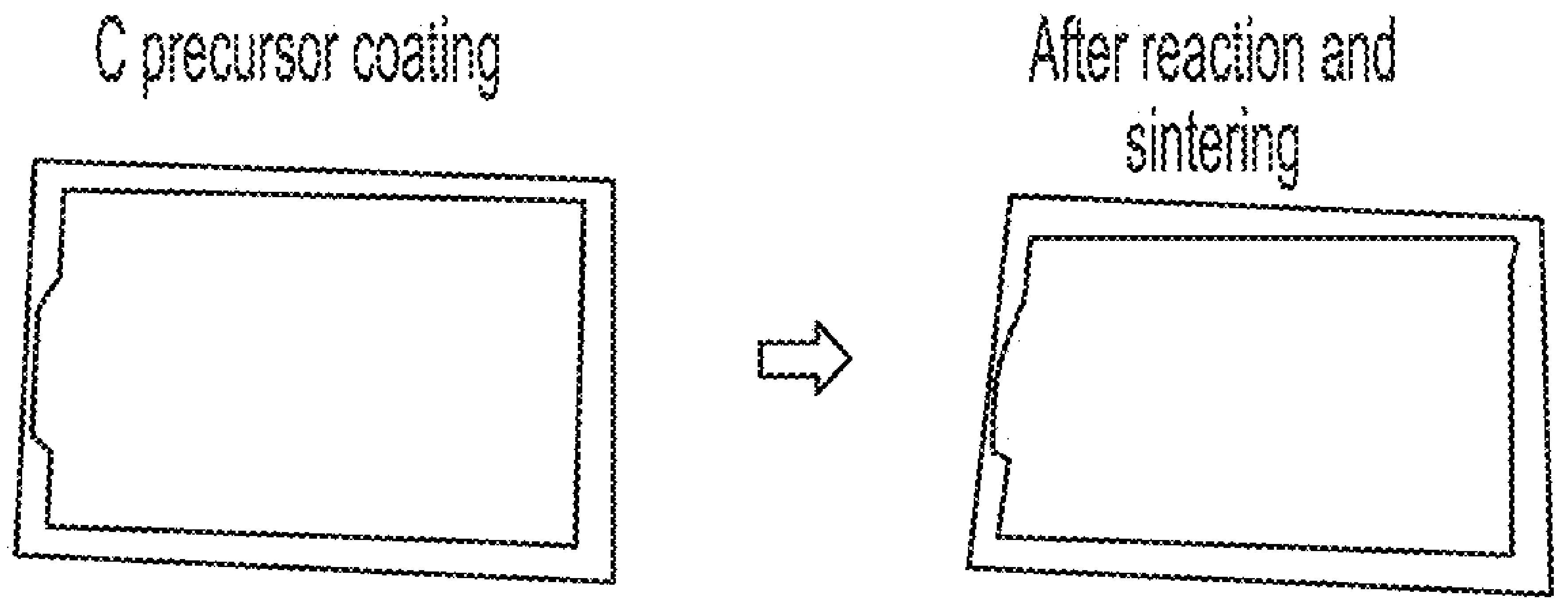

FIG. 15A

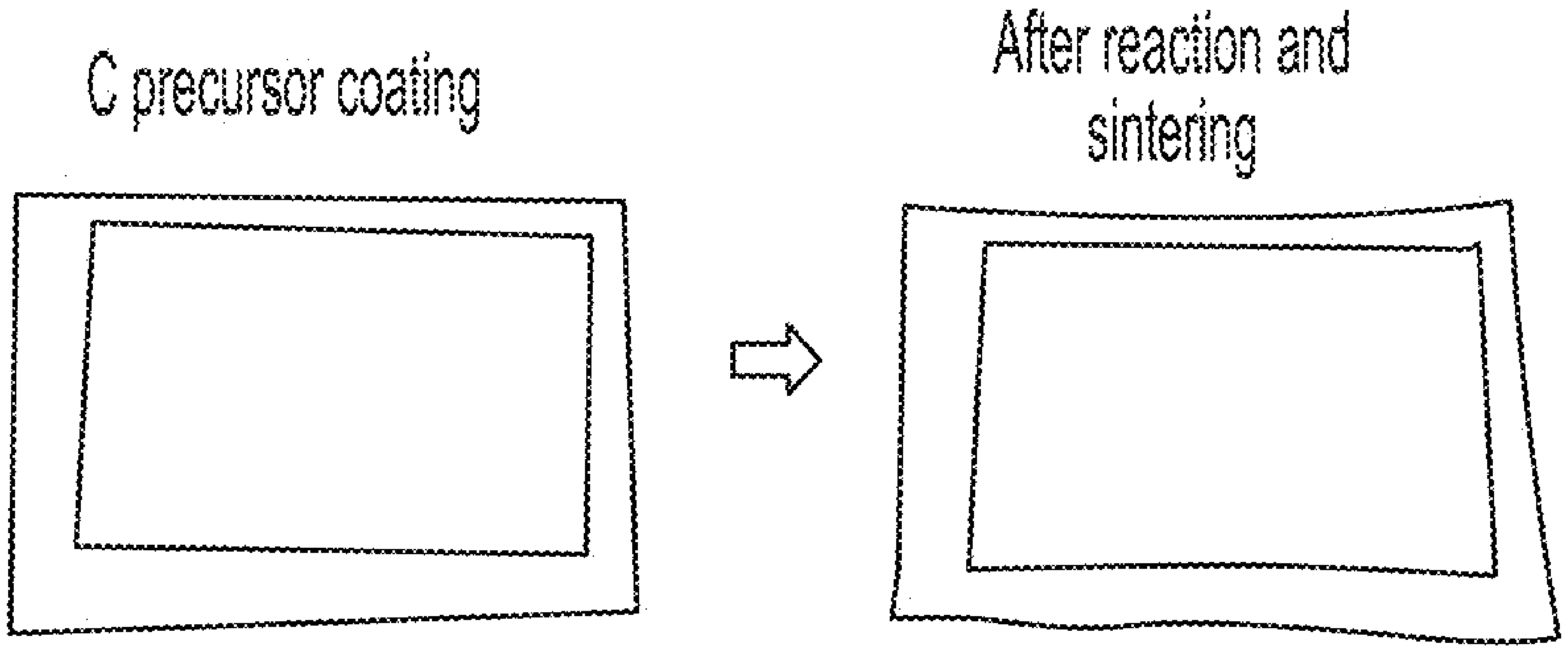

FIG. 15B

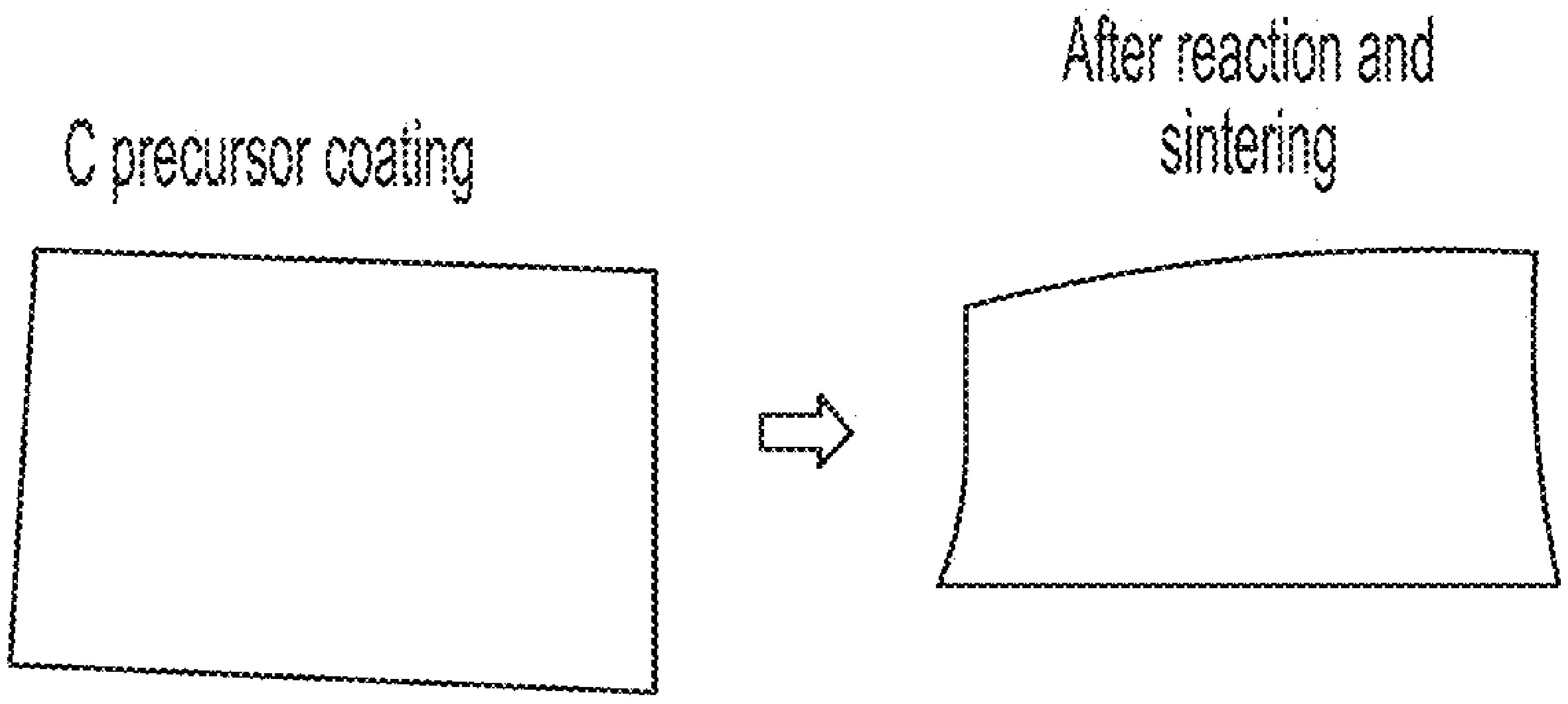

FIG. 15C

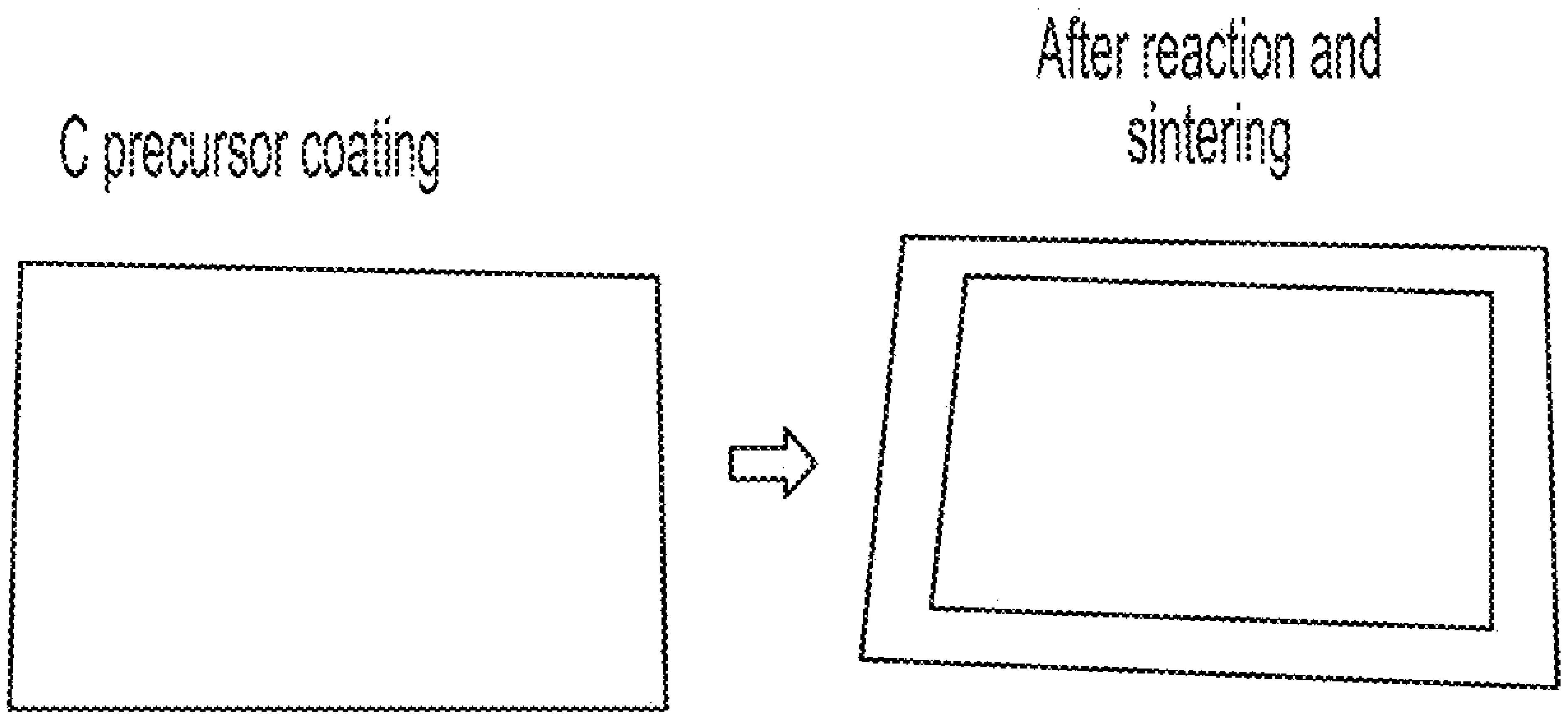

FIG. 15D

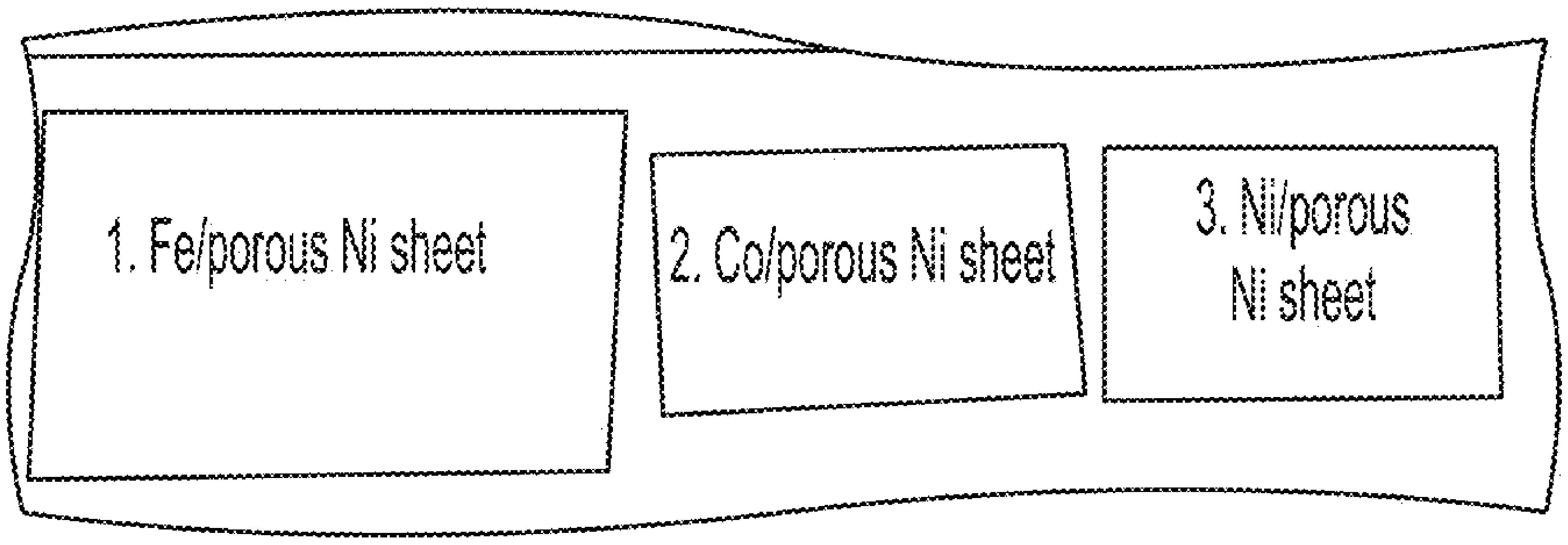

FIG. 16A

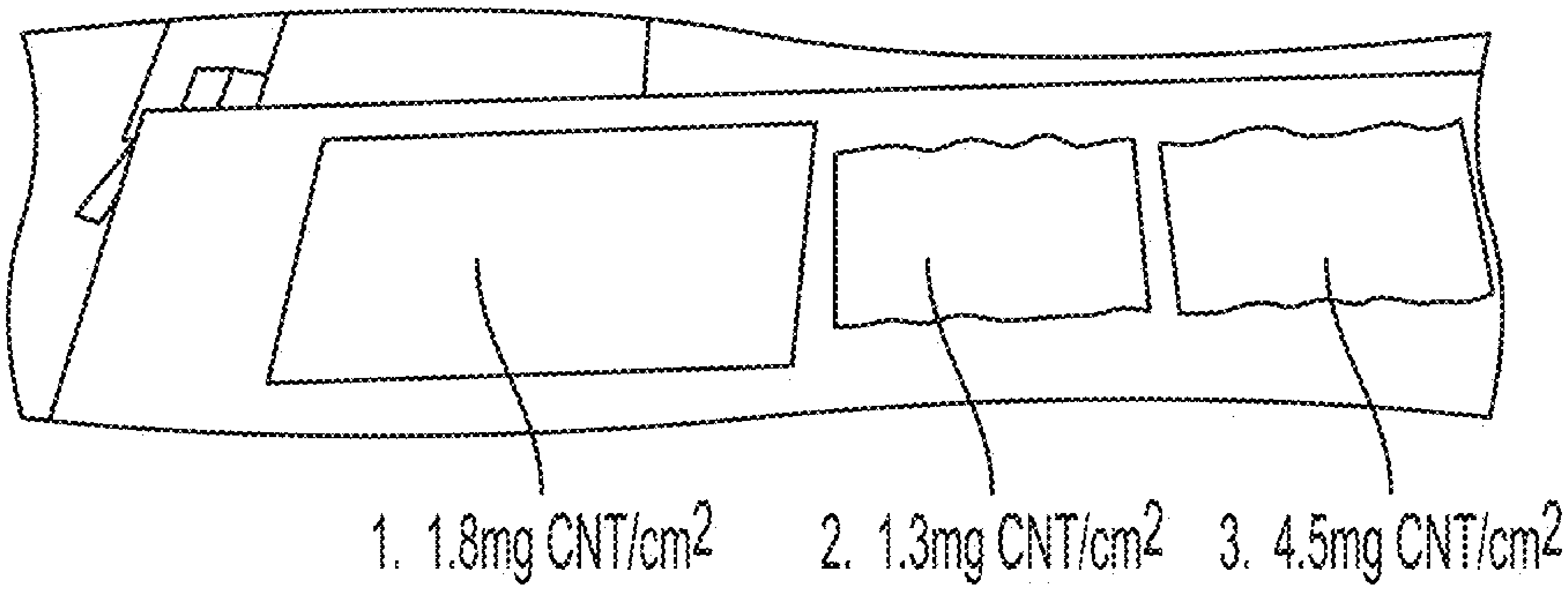

FIG. 16B

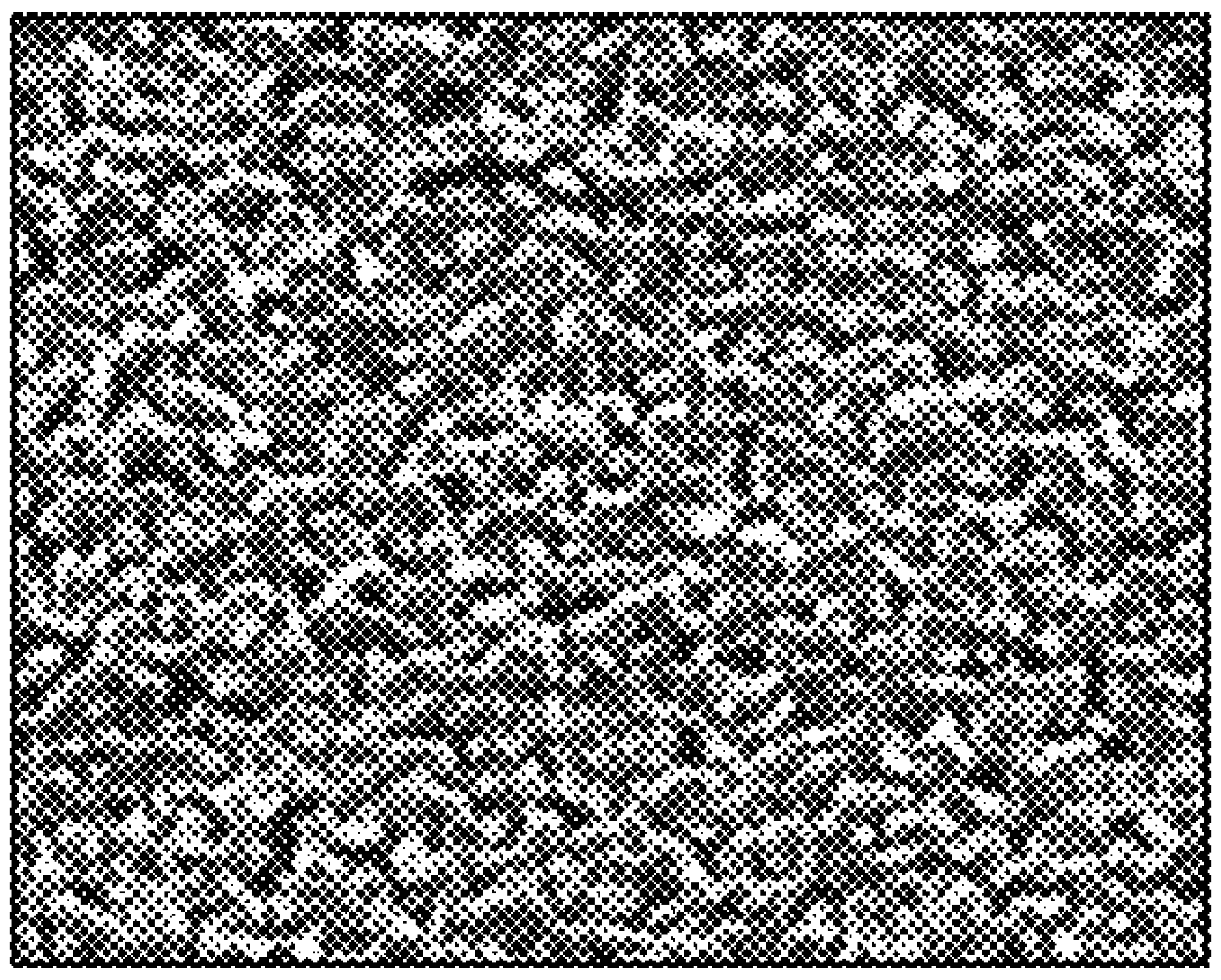

FIG. 17A

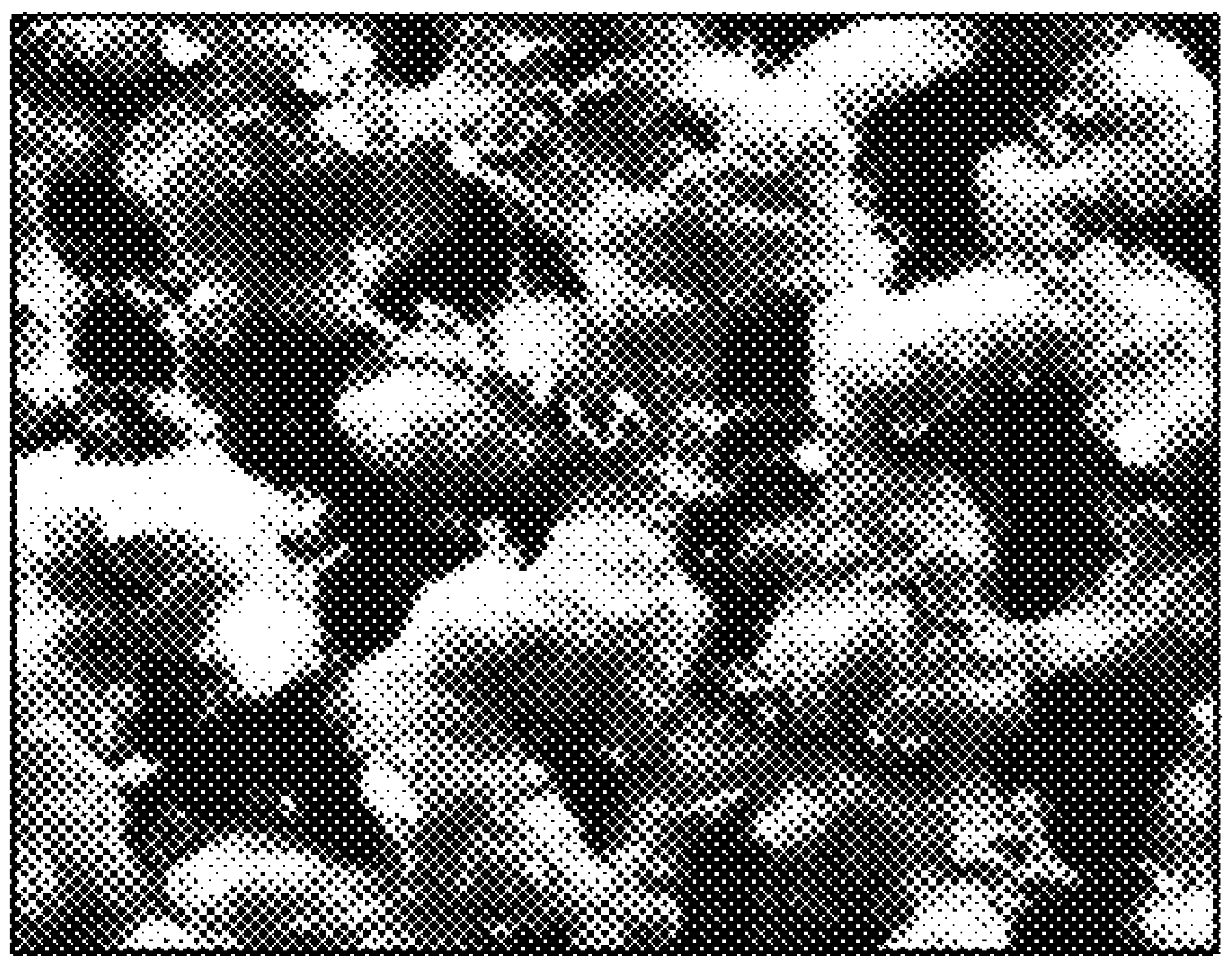

FIG. 17B

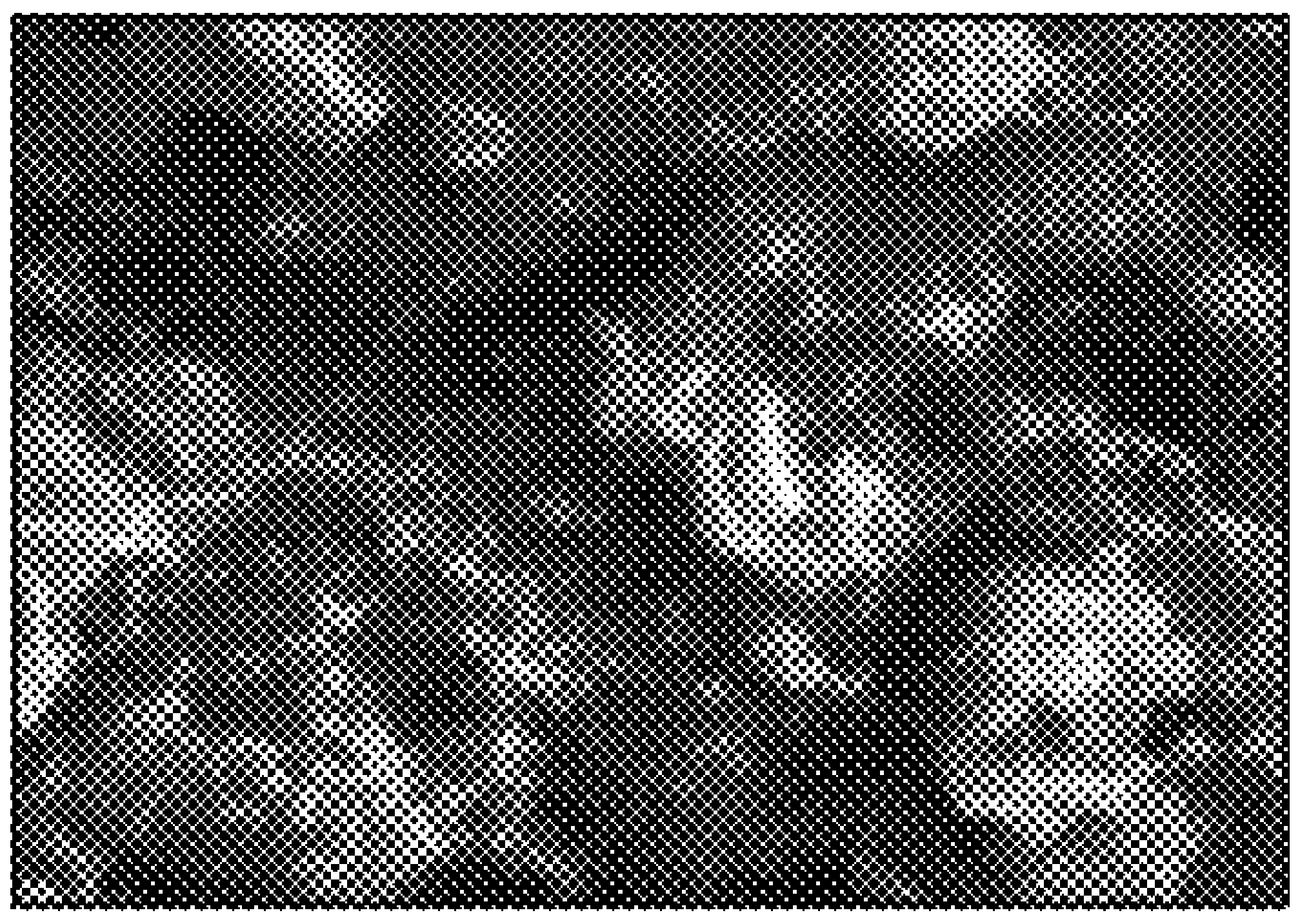

FIG. 17C

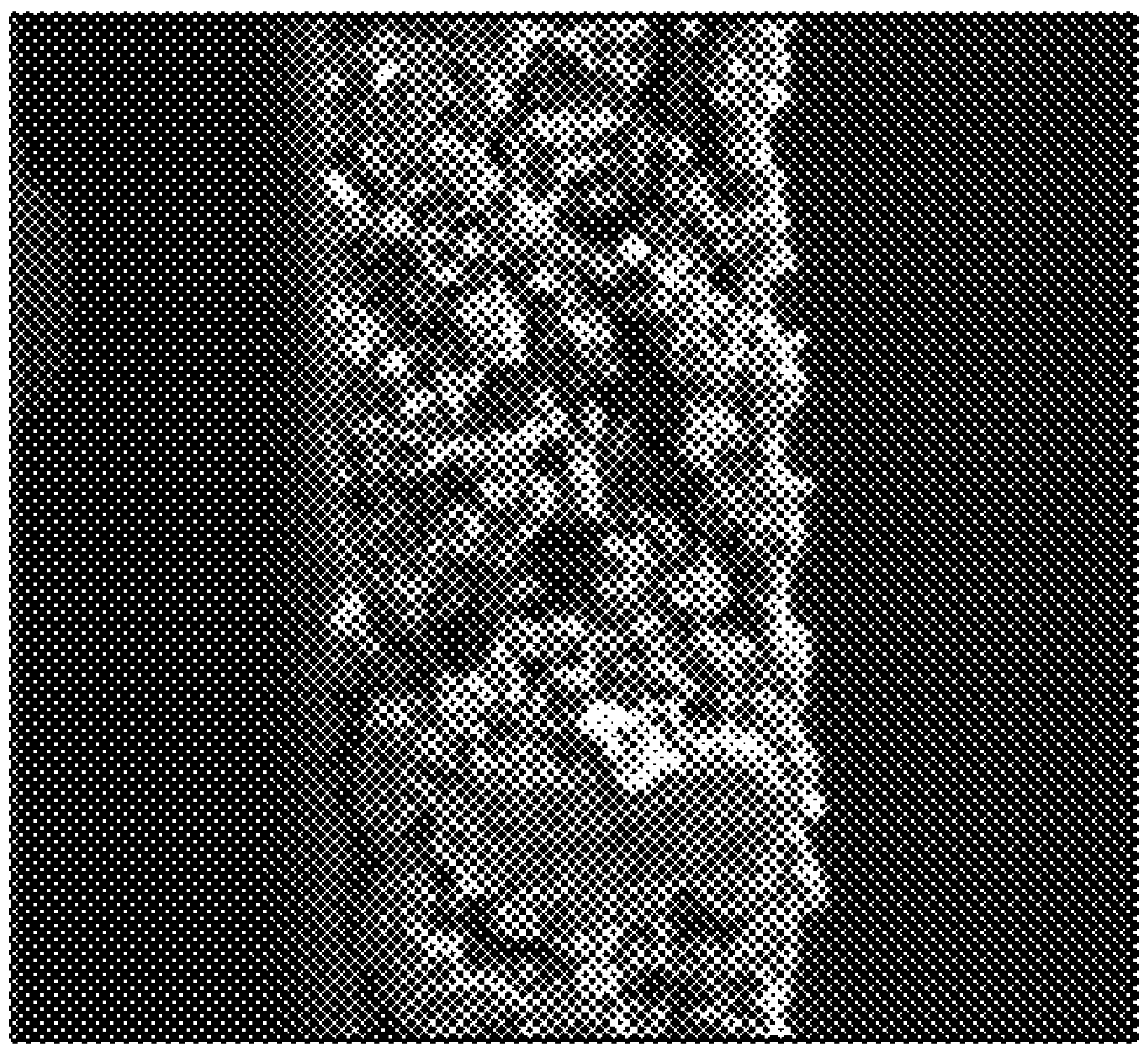

FIG. 17D

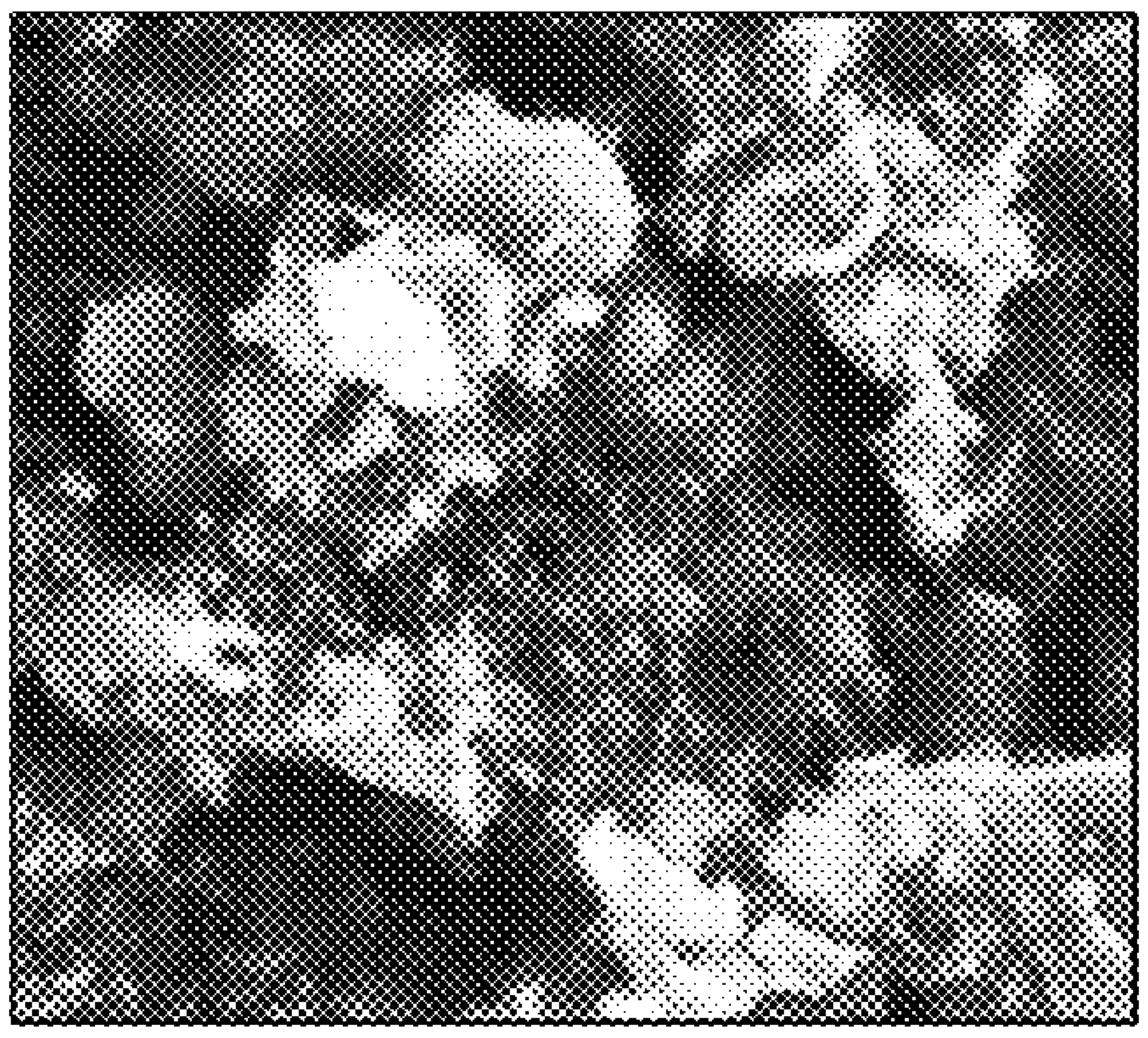

FIG. 17E

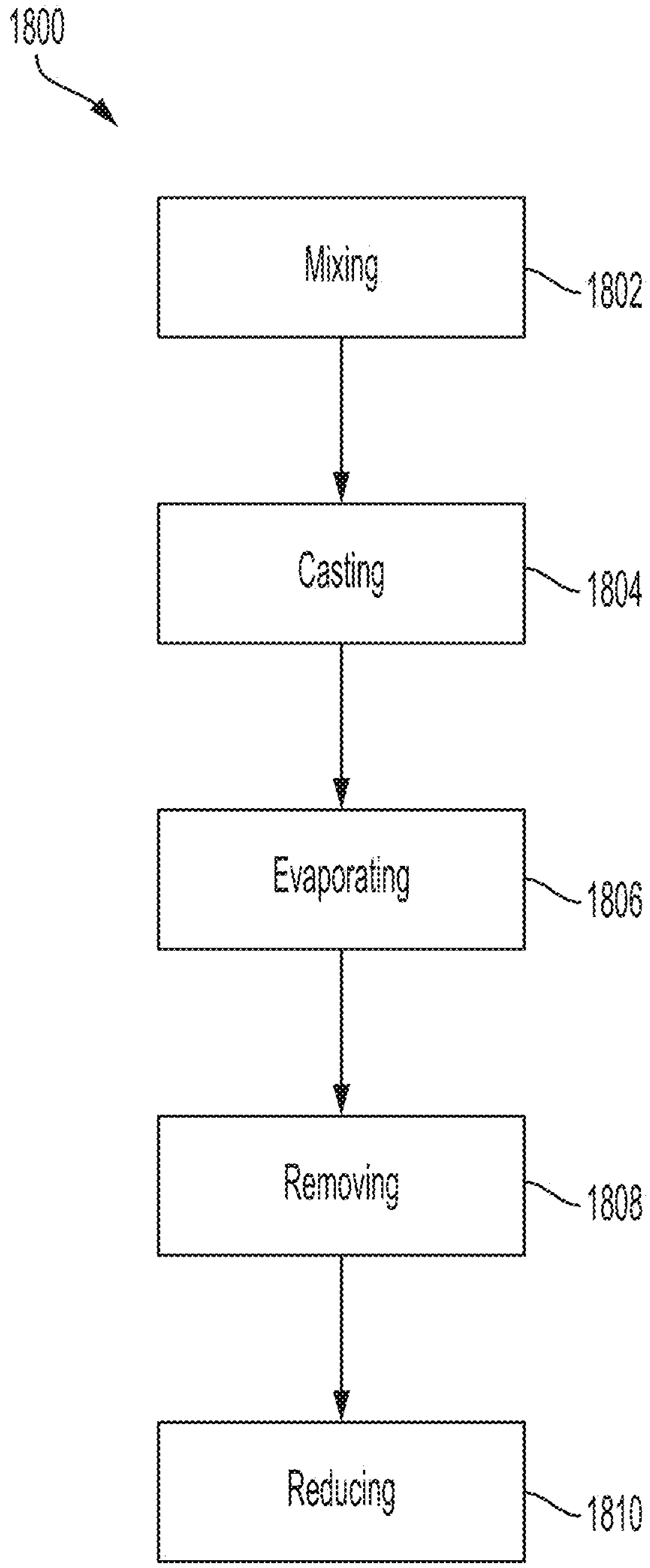
1800
Mixing
1802
Casting
1804
Evaporating
1806
Removing
1808
Reducing
1810

FIG. 18

PROCESS AND APPARATUS FOR CONTINUOUS PRODUCTION OF POROUS STRUCTURES

CROSS REFERENCE TO RELATED PATENT APPLICATION

[0001] This application is a Divisional of U.S. patent application Ser. No. 16/235,178, filed Dec. 28, 2018, which claims the benefit of U.S. Provisional Application No. 62/675,341, filed May 23, 2018, both of which are hereby incorporated herein by reference in their entirety for all purposes.

ACKNOWLEDGEMENT OF GOVERNMENT SUPPORT

[0002] This invention was made with government support under Contract No. DE-AR0000650 awarded by the U.S. Department of Energy. The government has certain rights in the invention.

FIELD

[0003] The present invention is directed to devices and methods for producing porous structures.

BACKGROUND

[0004] Micro-porous structures have a variety of applications, including molecular separation, particulate filtration, adsorption and absorption, catalytic reaction, conductive electrodes, membrane separator, acoustic absorption, impact and high-energy absorption, sensors, actuators, and hybrid composite materials. Metal-based structures provide some unique performance attributes compared to other materials. For example, metals possess much higher electrical and thermal conductivity than ceramics and polymers; metals are ductile compared to fragile ceramics; metals provide higher mechanical strength and thermal stability than polymers. Many commercial products with metal-based structures having pore sizes above about 10 micrometers are produced, such as screens and meshes, foams and sponges, and sintered filters. However, metal-based structures with pore sizes smaller than 10 um are expensive to make at large industrial scales.

[0005] The specific surface area of a porous structure increases with decreasing pore size in inverse first order. A high specific surface area is desired by applications for which large surface area is desirable, such as adsorption, catalytic reaction, and porous electrodes. The porous structures of pore sizes at micro- and sub-micrometer level can be used to filter fine particulates that are difficult to separate by other methods, such as filtering of bacteria, virus, and soot in fossil fuel combustion exhaust. The porous metal structures of pores at sub and micrometer scale can also be used as a support to prepare high-flux thin membranes of much smaller pore sizes, such as molecular sieve membranes of pores from 0.3 to 2.0 nm. The metal-based porous structures can be produced by powder metallurgy technologies at industrial scales from fine metallic particles. The metal particles, with addition of some binders and/or pore formers, can be made into various desired shapes (plate, tube, capillary, monolith) and sintered to form porous structures. The resulting pore size generally decrease with decreasing size of the metallic particle used. However, fine metallic particles are expensive to purchase and can become explosive when the particles become too small. Thus, using fine metal particles to produce porous structures is an expensive process.

SUMMARY

[0006] Embodiments herein disclose a continuous reactive process for production of porous metal-based structures of pore sizes ranging from 0.3 nm to about 5 μm from a green part having a characteristic pore diffusion mass transfer dimension less than 1 mm. The process comprises i) continuously feeding the green part and gas flow into a reactor of high aspect ratio, such as environment-controlled tunnel furnace; ii) moving the green part through the reactor which is heated with a designated temperature profile long the length, where the green part is reacted and converted into a product part of the designated porous structures under continuous gas flow; and iii) cooling down the product part and moving it out of the furnace. In the reactive conversion process, mass transfer plays a role in formation of the designated porous structure.

[0007] The characteristic diffusion mass transfer dimension is the dimension of a green part that is desirable for formation of the designated porous structures, where gaseous reactants and/or products transport into or out of the green part through diffusion. For example, for a green part in a sheet form, the characteristic dimension is the sheet thickness. For a green part in a tubular for, the characteristic dimension is the wall thickness. For a green part in a monolith form, the characteristic dimension is the channel wall thickness. If the green part is a coating on the preformed porous support, the characteristic dimension is the coating layer thickness.

[0008] For well-defined pore shapes such as a cylindrical pore, the pore size is its diameter. However, there are different ways to characterize the size of the pore of irregular shapes. One quick assessment commonly used in the field is to use the width for nearly square-shaped pores, the diameter for nearly rounded pores, and the spacing between two narrow sides in slit or rectangle kind of pores. Hydraulic diameter, as defined in fluid mechanics, can be calculated for any shape of pores and used as the pore size. Microscopy analysis provides direct observation and assessment of the pore size and shape. Mercury porosimetry is a well-established experimental method to quantify exterior pore size of a porous structure over a range of about 0.1 to 100 μm. For pore sizes in the range of 0.3 nm to 100 nm, gas adsorption and desorption is an established method to quantify the pore size.

BRIEF DESCRIPTION OF THE DRAWINGS

[0009] FIG. **1** is a drawing illustrating the conversion of a green part of metal oxide particles to a micro-porous metallic structure according to an embodiment.

[0010] FIG. **2** is a plot of particle size distribution of nickel oxide used to make a green tape according to an embodiment.

[0011] FIG. **3** is a plot of the reactivity of green tapes by TGA in H_2/Ar gas according to an embodiment.

[0012] FIG. **4** is a plot illustrating evolution of gaseous molecules during reaction of nickel oxide green tape in hydrogen according to an embodiment.

[0013] FIG. **5** is a drawing illustrating a green part of a supported coating to a micro-porous membrane or film according to an embodiment.

[0014] FIGS. **6**A and **6**B are diagrams illustrating the preparation of additional porous structures on a precursor or promoting material deposited on a porous support structure, wherein FIG. **6**A illustrates precursor or functional material supported on a porous structure as a film according to an embodiment and FIG. **6**B illustrates precursor or functional material deposited inside pores of a support structure according to an embodiment.

[0015] FIG. **7** is a schematic illustration of an apparatus for continuous production of micro-porous structures according to an embodiment.

[0016] FIG. **8** is a plot illustrating the temperature profiles of three reactor sections of a tunnel furnace according to an embodiment.

[0017] FIGS. **9**A-**9**C are photographs illustrating the morphologies of green tape and porous metal sheet produced according to an embodiment; where FIG. **9**A illustrates the green tape, FIG. **9**B illustrates a metal sheet produced on the support plate and FIG. **9**C illustrates a self-supported thin metal sheet.

[0018] FIGS. **10**A and **10**B are plots illustrating the tunnel furnace temperature profiles used for conversion of nickel oxide green tapes into porous nickel alloy sheets according to an embodiment.

[0019] FIGS. **11**A-**11**C are SEM micrographs illustrating the microstructure at various magnifications of porous metal sheets produced according to an embodiment.

[0020] FIG. **11**D is a plot illustrating the surface pore size distribution of the sheet illustrated in FIGS. **11**A-**11**C.

[0021] FIGS. **12**A and **12**B are photographs illustrating the morphologies of micro-porous ceramic coatings on the thin porous metal sheets according to an embodiment.

[0022] FIGS. **13**A-**13**D are SEM micrographs illustrating structures of a 200 nm YSZ coating on the thin porous metal sheet at different magnifications according to an embodiment. FIG. **13**D illustrates an elemental mapping of the coating.

[0023] FIGS. **14**A and **14**B are SEM micrographs of structures of a 50 nm/200 nm YSZ coating on a thin porous metal sheet at different magnifications according to an embodiment. FIG. **14**B illustrates an elemental mapping of the coating.

[0024] FIGS. **15**A-**15**D are photographs illustrating the conversion of carbon precursor coatings on the porous metal-based supports into micro-porous carbon films according to an embodiment.

[0025] FIGS. **16**A-**16**B are photographs illustrating morphologies of three porous Ni sheet coupons functionalized for carbon nanotube growth according to an embodiment.

[0026] FIGS. **17**A-**17**E are SEM micrographs under different magnification illustrating carbon nanotubes grown inside pores of a porous Ni sheet.

[0027] FIG. **18** is a flow diagram of a method of making porous structures according to an embodiment.

DETAILED DESCRIPTION

[0028] The following description includes the preferred best mode of one embodiment of the present invention. It will be clear from this description of the invention that the invention is not limited to these illustrated embodiments but that the invention also includes a variety of modifications and embodiments thereto. Therefore, the present description should be illustrative and not limiting. While the invention is susceptible of various modifications and alternative constructions, it should be understood, that there is no intention to limit the invention to the specific form disclosed, but, on the contrary, the invention is to cover all modifications, alternative constructions, and equivalents falling within the spirit and scope of the invention as defined in the claims.

[0029] FIGS. **1-6** show three embodiments of the present invention. In the conversion process illustrated in FIG. **1**, a green part body **100** comprising particles of metal precursors such as metal oxides, pore formers and organic additives is converted into a porous metallic structure **102** in hydrogen gas environment through the following reactions:

[0030] Organic additives+H_2→vapor

[0031] Pore former+H_2→vapor

[0032] Metal precursor (oxide)+H_2→Metallic grain (solid)+vapor

[0033] Metallic grains (solid)→Networked porous structures

TABLE 1

Typical composition of green tapes

	Wet slurry tape, Wt. %	Tape dried, Vol. %
Metal oxide	52	33
Pore former	14	33
Solvent	25	0
Dispersant	1	4
Binder	5	18
Plasticizer	3	12

[0034] Compositions of the green part are illustrated with the green tape cast from slurry comprising metal oxide particles in table 1. Particle size distribution of the metal oxide such as nickel oxide used to make the slurry is shown in FIG. **2**. The particle size may be in a range of 0.1 to 4 μm with 50% of the particles below 0.35 μm and 95% particles below 1.54 μm. FIG. **18** illustrates a flow diagram of an embodiment of a method **1800** of making porous structures from a slurry. In a first step, **1802**, the metal oxide particles are mixed with a carbon black pore former, dispersant, organic binder, solvent and plasticizer into homogenous slurry in an organic solvent. Next, the slurry is cast into a green tape of about 70 μm thickness, step **1804**. Then, the solvent is evaporated during casting to form a nearly dense green tape, step **1806**. In the next step (step **1808**), the non-volatile organic additives and pore formers are removed from the green part into vapor phase by pyrolysis, cracking, and/or hydrogenation reactions. Removal of these constituents in the green part leaves voids or pores **104** in the part. The metal precursor such as metal oxide is reduced into metallic grains. The gaseous species released from those reactions are swept away by a gas flow. Networked porous structures are formed by controlling the degree of sintering of these metallic grains (step **1810**).

[0035] The pore size is mainly determined by particle size of the metal precursors. By using fragile precursor materials such as metal oxides, the particle size over a range of 100 nm to 5 μm can be produced by milling of bulk powder materials. Metallic materials are too ductile to be milled into such small sizes. The pore size in the resulting porous metal structure made from the fragile precursor materials can be smaller than the precursor particle size due to shrinkage of the metal precursor particle. For example, the density of nickel oxide is 6.67 g/cc, while the density of nickel metal is 8.89 g/cc. The porosity is mainly determined by volume fraction of the pore former in the green part. The pore former, as a sacrificial material, is preferably in-expensive and removable under the reaction conditions. The preferred pore former materials are carbon blacks, polymer particles, and carbonate particles. The organic additives, including dispersant, binder, and plasticizer, are used to make the metal precursor particle into desired shapes. They are typically organic materials.

[0036] Reactivity of the green part **100** can be characterized by thermogravimetric analysis (TGA). Weight changes of four different metal oxide green tapes processed by programed heating in hydrogen/argon gas flow are shown in FIG. **3**. The NiO tape **1** was made of nickel oxide particle and carbon black pore former, while the NiO tape **2** was made of the same nickel oxide but with a carbonate pore former. The oxide composite tapes were made of Ni—Fe—Cr mixed oxides and the carbon black pore former. The composite tapes **1** and **2** are made of mixed oxides of the same composition but prepared in two different ways. The sample was heated from ambient 25° C. to 650° C. at a ramp rate of 5° C./min and held isothermally at 650° C. for 2 hours. The weight loss started at about 220-240° C. First stage of rapid weight loss occurred between 320-400° C., which corresponds to pyrolysis of the organic additives and reduction of metal oxides. Second stage weight loss started at about 500-600° C., which corresponds to decarbonation. The green parts **100** of different compositions show some variation in the extent of weight loss and starting temperature. But, the green parts **100** exhibit common characteristics in removal of some constituents in the green part into vapor phase by chemical reactions.

[0037] The reactivity of the green part **100** can be further delineated by heating the sample inside a furnace with pure hydrogen gas flow. FIG. **4** shows evolution of gaseous reaction products, H_2O, CO_2, C_2H_6, CH_4, and CO during programed heating of a nickel oxide green tape in pure hydrogen gas from 20 to 835° C. Peak production of H_2O, CO_2, CH_4 and C_2H_6 occurs in the temperature range of 200 to 400° C., which corresponds to a slight dip in hydrogen signal. H_2O production is attributed to reduction of nickel oxide. Production of CH_4 and C_2H_6 results from pyrolysis and cracking of the organic additives. CO_2 formation can be explained by reaction of the organic additive with nickel oxide. The second peak production of CH_4 occurs in the range of 550 to 700° C., which results from reaction of hydrogen with the carbon pore former. Small amounts of CO were also produced during the process. Evolution of these gaseous products clearly shows the kinds of chemical reactions involved in decarbonization and deoxygenation of the green part for formation of sintered porous metallic structures.

[0038] In the reactive conversion process illustrated in FIG. **5**, the green part **100** is in the form of coating or film **502** supported on a pre-formed porous support structure **504**. The coating layer **502** comprises packing of preformed particles/grains **506** with organic additives **508** and/or sintering promoters **510** at a thickness less than 40 μm. The support pore size is about 200 nm to 5 μm. Examples of the preformed particles **506** include stable ceramic crystalline materials, such as zirconia, alumina, ceria, and silicon carbide. These preformed particles **506** may be impregnated or doped with some promoter **510** to facilitate sintering of the preformed particle **506** from point-to-point contact to neck-to-neck bonding. Organic additives **508** such as dispersants and binders are incorporated into the green part **100** in the coating process. The preformed particle size is substantially smaller than the size of the support pores **512**, by a few times to one order of magnitude, to form a membrane layer **514** having membrane pores **516** with pore sizes in the range of 5 to 100 nm. in an embodiment, the coating layer **502** may be formed by multiple coatings with different particles sizes in an order of decreasing particle size from the support to surface. The support structure **504** is intact or experiences minimal changes during the membrane formation process. The support structure **504** is preferably made of metallic backbones.

[0039] Sintering of porous ceramic coatings on a porous ceramic support by high-temperature heating in an oxygen-containing gas environment is known in the membrane field. For example, porous zirconia membranes supported on a porous alumina tube can be sintered by heating at above 1000° C. in air. However, sintering of a durable ceramic-type membrane **514** on a metal-based support structure **504** is extremely challenging. The metal support structure **504** can be damaged or destroyed by heating above 500° C. in a O_2-containing gas environment. Even in an inert or reducing gas environment, the porous metallic support structures **504** can experience significant shrinkage at high temperatures. A decarbonization and sintering process with controlled temperature gradient and gas environment is provided herein to form a micro-porous ceramic membrane on the preformed metal-based support structure **504**:

[0040] Organic additives+H_2→vapor

[0041] Packed particles or grains (+promoter)+H_2→Vapor+sintered grains

[0042] The non-volatile organic additives **508** incorporated in the green part **100** during the coating process are removed into the vapor phase by pyrolysis, decomposition, cracking, and/or hydrogenation. The sacrificial material introduced in pre-reforming of the coating particles with addition of the sintering promoter **510** is removed as well during sintering of the grains.

[0043] Additional porous structures may be formed out of a green part **602** comprising dense or less porous material supported on a porous support structure **504** as illustrated in FIGS. **6**A and **6**B. FIG. **6**A show conversion of a dense or less porous coating layer **602** on a porous support structure **504** into a networked porous structure **604** through solid/vapor reactions. For example, a carbon precursor can be coated on the support structure as a dense or less-porous layer at low temperatures (<100° C.) and may be converted into micro-porous carbon film by chemical reactions at high temperatures (500-900° C.).

[0044] The carbon precursor+gas→porous carbon+gaseous by-products

[0045] The pores **604** are generated by removing a fraction of the carbon in the green part **602**. In an embodiment, the carbon precursor material can be phenolic resins and furthermore, thermoset-type phenolic resin, in which oxygen atom in the precursor material can act as an in-situ reactant to generate porous structures. CO_2 gas may be added to react with the carbon to form CO. H_2O vapor may be added to react with the carbon to form H_2 and CO. Hydrogen gas can be used to react with carbon to form methane.

[0046] Another example is formation of a micro-porous silicone carbide film or membrane **604** by reacting a functionalized film **602** on the support **504** with carbosilane-type vapor at temperatures of 500-900° C.:

[0047] Functionalized film/support+Carbosilane→micro-porous SiC film/support+gaseous by-products

[0048] The carbosilane is a source of C and Si atoms to form silicone carbide. The support is functionalized, forming a functionalized coating **602**, to promote, direct, and/or catalyze deposition and reaction of gaseous carbosilane on the support **504** to form a porous silicone carbide film **604**. For example, the support **504** can be functionalized by impregnation or coating of alumina of particle sizes less than 100 nm. Similarly, a micro-porous silica membrane or film **604** can be formed by the gas/solid reaction with a vapor-phase precursor containing Si and O atoms:

[0049] Functionalized support+Si&O precursor→micro-porous silica film/support+gaseous by-products

[0050] Examples of the Si and O-containing precursor include vinyltriethoxysilane (VTES) and tetraethoxyorthosilicate (TEOS). In this conversion process, the support can be functionalized by coatings of alumina of particle size less than 100 nm. A small fraction of Ni, Fe, and/or Co may be added into the coating.

[0051] The new porous structures can be formed inside the pores of a porous support structure. As shown in FIG. **6**B, surface of the metallic grains inside a porous metal-based support structure may be functionalized, such as by deposition of a catalyst to form a functionalized support **606**. Under the reactive conditions, a gas reactant diffuses into the pores **512** of the support to form new structures **600**. Such a process is illustrated with growth of carbon nanotubes inside the support pores:

[0052] Functionalized support+Carbon precursor→Carbon nanotubes+gaseous by-products

[0053] The metal-based porous support can be functionalized by deposition of transition metal catalysts, such as Fe, Ni, and/or Co, on the surface of metallic grains inside the support. The carbon precursor can be, but is not limited to, CO, methane, ethanol, ethane or ethylene in an inert carrier gas such as nitrogen. The chemical vapor deposition or gas/solid reaction may be carried out at temperatures from 500 to 900° C.

[0054] The common features of above-described formation processes of micro-porous structures are i) reaction of gaseous reactant with the green part at high temperatures (500 to 1200° C.), ii) evolution of gaseous byproducts, and iii) reducing or inert gas environment with substantial absence of oxygen gas. The reaction temperature should be well controlled to achieve the designed level of reaction conversion. The gaseous reactant should be constantly supplied and the gaseous byproducts should be constantly removed. Therefore, a continuous production process is presented by this embodiment to produce the porous structures economically at large scales. The porous structures can be in various forms or shapes, such as sheets, tubes, and monoliths. A flat sheet form is preferred, because its simple geometry renders high throughput handling. Furthermore, the sheet thickness is preferably thin, less than 1 mm or less than 200 μm. The thinness of the sheet reduces diffusion mass transfer resistance and increases stacking density of the sheets. The basic functional units of a continuous production system **700** are shown in FIG. **7**. The green parts **100** located on supports **504** are fed into an inlet gas exchange chamber **702** where oxygen or air entrained into the chamber is removed, such as by sweep with an inert gas. The green parts **100** are moved into a preheating section **708** via a gas-tight connector **704**. In the preheating section, volatile or thermally-unstable constituents in the green parts are removed via an exhaust outlet **706**. Then, the green parts **504** are moved into a reaction and sintering section **710** where the green parts **504** react with a gas flow, provided via a gas inlet **714**, to form product parts **718** of desired porous structures. The product parts **718** are moved into cooling section **712**. After the product parts **718** are sufficiently cooled down, the product parts **718** are moved into an outlet gas exchange chamber **716** where the reactive gas entrained by the product parts **718** are removed, such as by sweep with inert nitrogen gas. The green parts **100** are continuously fed while the product parts **718** are continuously moved out. The reactive gas is continuously introduced into the reaction and sintering section **710** to purge the gaseous products out of the furnace and supply the reactant to react with the green part **100**, while the reacted gas stream is continuously discharged. The feed gas may be introduced at different locations or sections, while the reacted gas may be discharged at different locations or section. For example, the feed gas may be introduced at the cooling section **712**, reaction and sintering section **710**, and the preheating section **708** to meet specific needs to the gas flow rate and compositions in respective sections **708**, **710**, **712**. The gas flow direction is preferably opposite to the moving direction of the green parts **100**. The feed gas composition is determined by specific reaction conversion need. If conversion of the green parts to the product parts **718** is limited by hydrogen reaction, pure hydrogen is used. If the conversion requires a small fraction of active reactants, such as CO_2, H_2O, CO, ethanol, CH_4, carbosilane, or TEOS, an inert carrier gas, such as nitrogen, argon and Helium, can be used. One feature of the present system **700** is that the feed gas should be substantially free of oxidants, such as oxygen, to protect the formed porous structure **718** from being oxidized.

[0055] The preheating **708**, reaction and sintering **710**, and cooling sections **712** may be built as mutually-connected individual sections or as different zones in one reactor body. The three sections are controlled with different temperature profiles. As illustrated in FIG. **8**, the green part **100** is heated from ambient temperature to moderate temperatures such as 200-400° C. in the preheating zone **708**. In the reaction and sintering zone **710**, the green part **100** may be heated to and held at much higher temperatures. For example, the temperature is as high as 1000-1300° C. for formation of micro-porous stainless-steel structures. The temperature required for formation of porous nickel and nickel alloy is about 750 to 900° C. For sintering of porous ceramic coatings on a porous metal structure, the temperature is about 700 to 1100° C. For formation of micro-porous carbon membrane, silica membrane, silicone carbide membrane or growth of carbon nanotubes, the temperature is about 500 to 900° C. The reaction and sintering section **710** should have sufficiently high aspect ratio to control the temperature profile. The aspect ratio is defined as ratio of the reactor length to width of the reaction tunnel or diameter for a rounded reaction channel. The aspect ratio is preferably greater than 2.

Example I: Conversion of Nickel Oxide Green Tapes into a Thin Porous Metal Sheet

[0056] A green tape comprising nickel oxide particles was converted into thin porous Ni alloy sheets in a continuous tunnel flow reactor. The green tape thickness was about 70 μm with the composition listed in Table 1. As shown in FIG. **9**A, the thin green tape **900** is flexible enough to be wrapped on a roller **902**. The green tape **900** was cut into 35 cm×35 cm coupons and set on a durable substrate plate to be processed in a tunnel flow reactor or environment-controlled tunnel furnace. The tunnel furnace temperature was maintained by use of many independently-controlled electrical heaters along the furnace length. FIG. **10** shows the temperature profiles in the three sections. In the pre-heating section (FIG. **10**A), the temperature was gradually increased to 400° C. through nine heating zones. In the reaction section (FIG. **10**B), the temperature was raised from 400° C. to 810° C. in six heating zones. The temperature was dropped from 810° C. to 200-300° C. in only three heating zones in the cooling section **712**. In the preheating, reaction and sintering sections **708**, **710**, the temperatures in lower and upper points of the tunnel were maintained almost the same to achieve uniform de-gas, reaction, and sintering over the cross-section of the tunnel. The green tapes **900** were continuously moved through the tunnel and experienced significant temperature variance along the tunnel length. The de-gas, reaction, and sintering rates should be well controlled and balanced to prevent formation of defects, such as cracks, wrinkling, and pinholes. After the porous metallic structure **102** is formed, the porous metal sheet **102** can tolerate a larger degree of temperature variation. Thus, the temperature gradient among two heating zones can be much greater in the cooling section than in the preheating **708** and reaction sintering **710** sections. Pure hydrogen gas was introduced into the reactor tunnel at end of the cooling section and discharged at the beginning of the preheating section **708**, i.e., the hydrogen flow direction was opposite to the green part movement. After the desired temperature profiles and hydrogen gas flow were stabilized, stacks of the green tapes were pushed into the preheating section **708** and pushed out of the cooling section **712** continuously one by one.

[0057] FIG. **9**B shows a thin porous Ni alloy sheet **718** produced from the continuous furnace. The thin sheet **718** was laid on a rigid and stable substrate plate. The sheet **718** looked flat and free of any defects. The thin metal sheet **718** presents much higher strength than the green tape **502**. FIG. **9**C shows that the porous metal sheet **718** is strong enough to be self-supported. No light penetration or pin-holes are seen on the sheet **718**. Any holes that allow the light to go through indicate that the hole is too large. In the continuous production process, the stacks of green tapes **502** are fed into the tunnel reactor one by one or stack by stack. Sizes and porosity of a few consecutive stacks processed under the same conditions are summarized in table 2. The average thickness and porosity of these stacks listed in Table 2 are 46±2 μm and 40±3%, respectively. These variances are acceptable to most practical applications.

TABLE 2

Porous thin Ni sheets produced by a continuous process

Stack	Width, cm		Thickness, μm		Geometric
#	Avg.	STDEV	Avg.	STDEV	Porosity
1-2	23.7	0.1	44	3	0.44
1-3	23.3	0.1	45	2	0.43
1-4	23.4	0.3	44	2	0.41
1-5	23.4	0.2	45	3	0.43
1-6	23.7	0.1	44	1	0.43
2-1	23.9	0.3	44	1	0.43
2-2	23.4	0.2	46	2	0.43
2-3	23.5	0.2	43	2	0.43
2-4	23.4	0.1	44	1	0.42
2-5	23.5	0.1	44	2	0.42
2-6	23.4	0.2	47	2	0.44
3-1	23.7	0.1	46	2	0.45
3-2	23.2	0.3	45	1	0.41
3-3	23.1	0.1	44	2	0.40
3-4	23.3	0.1	45	1	0.41
3-5	23.5	0.1	45	3	0.42
3-6	23.5	0.1	45	2	0.42
5-1	23.0	0.2	44	2	0.38
5-2	22.5	0.2	44	2	0.36
5-3	22.5	0.2	46	1	0.38
5-4	22.6	0.2	44	2	0.36
5-5	22.6	0.1	45	2	0.38
5-6	22.5	0.1	46	2	0.37
5-7	22.4	0.1	45	0	0.36
5-8	22.5	0.1	47	3	0.38
6-1	23.0	0.2	44	2	0.38
6-2	22.4	0.1	47	1	0.37
6-3	22.3	0.1	47	2	0.37
6-4	22.4	0.1	48	2	0.39
6-5	22.6	0.2	47	2	0.39
6-6	22.4	0.2	47	2	0.38
6-7	22.5	0.2	47	1	0.38
6-8	22.6	0.1	46	2	0.37
8-1	23.5	0.1	48	1	0.44
8-2	23.0	0.2	49	3	0.43
8-3	22.8	0.1	47	2	0.40
8-4	22.8	0.2	49	1	0.42
8-5	22.8	0.1	47	2	0.40
8-6	22.8	0.4	46	1	0.38
9-1	23.5	0.4	47	2	0.42
9-2	22.8	0.2	46	3	0.38
9-3	22.6	0.2	47	3	0.38
9-4	22.6	0.2	50	3	0.42
9-5	22.7	0.2	48	3	0.41
9-6	22.8	0.2	49	3	0.42
10-1	23.6	0.3	48	2	0.44
10-2	22.9	0.3	49	1	0.41
10-3	22.6	0.2	49	4	0.40
10-4	22.6	0.2	50	3	0.41
10-5	22.5	0.2	48	2	0.37
10-6	22.6	0.1	47	2	0.39

[0058] The porous structures of the resulting metal sheet can be seen under electron scanning microscopy (SEM). FIGS. **11**A-C show scanning electron microscope (SEM) images under different magnification. At 100× magnification (FIG. **11**A), a smooth surface is seen, and pores are not visible yet. At 1000× (FIG. **11**B) magnification, the porous structure and surface features become evident. The image at 5000× magnification (FIG. **11**C) shows neck-to-neck sintering of metallic grains, pores or voids formed among the grains, and some carbon residuals. The porous surface structure looks uniform and no pore size greater than 5 μm are seen. FIG. **11**D shows the surface pore size distribution of two representative porous Ni alloy sheets produced in this embodiment. Consistent with SEM analysis, narrow pore size distribution is shown by both samples, although there is about 0.1 μm shift in the peak pore size. The pores are within the range of 0.4 to 2.0 μm, i.e., at the sub and micrometer scale.

Example II: Sintering of Micro-Porous Ceramic Coating on the Porous Metal Sheet Support

[0059] Two porous Ni alloy sheets produced from the continuous hydrogen furnace with respective thicknesses of 49±1.6 μm and 47±1.3 μm were used as a support structure **504**. They were cut into 3.5 cm×5.5 cm coupons for preparation of porous ceramic membranes of pore sizes much smaller than the support. The ceramic particles were coated on a 3.0 cm×5.0 cm area of the coupon by vacuum filtration of a coating slurry. The ceramic particle used for first layer coating was yttria-stabilized zirconia (YSZ) of 200 nm mean particle size. The YSZ particle was impregnated with 1.1 wt. % nickel oxide as a sintering promoter. The 1st coating slurry included 0.5 wt. % of the 200 nm YSZ solid, 0.013 wt. % of organic dispersant, and 0.013 wt. % of organic binder in isopropanol solvent. The slurry volume used for the first layer of coating is listed in table 3. The metal surface was fully covered by first coating to form a smooth, uniform coating layer. Then, second coating with 50 nm YSZ particles was applied. The second coating slurry included 0.25 wt. % of the 50 nm YSZ particle, 0.006 wt. % of the dispersant and 0.006 wt. % of the binder. The volume of the coating solution used is listed in table 3. The coated samples were dried in ambient air conditions. The amount of coating is normalized by the coated area as surface loading density, mg/cm^2. The as-coated layer, comprising stacking of the YSZ particles, was very loose such that it could be easily wiped or rinsed away from the support sheet. It should be sintered to form a stable structure.

TABLE 3

Micro-porous ceramic membranes supported on the thin porous metal sheet

ID No.	Metal sheet thickness, μm	Porosity, %	1st coating slurry usage, ml	2nd coating slurry usage, ml	Coating loading, mg/cm^2	Coating thickness after sintering, μm	Electrical conductivity
1	49	42	3	No	1.05	NA	NA
2	49	45	3	1	0.64	9	NA
3	49	47	3	1	0.79	2	Yes
4	49	45	3	1	0.77	3	Yes
5	49	47	6	2	1.57	NA	NA
6	49	43	6		1.67	5	Yes
7	49	44	6	2	1.61	5	Yes
8	49	44	5	2	1.82	6	NA
9	49	42	10	4	3.58	20	No
10	47	43	10	4	3.24	23	No
11	47	43	10	4	3.12	11	No
12	47	43	10	4	4.17	15	No
13	47	41	10	4	3.18	NA	NA

NA = not measured.

[0060] All the membrane coupons were placed on one support plate, fed into the continuous tunnel reactor, and sintered under the same conditions as the green nickel oxide tape described in the previous example. Morphologies of all the coupons before and after sintering are compared in FIG. **12**. As-coated samples looked white or pale, which reflects packing of the YSZ particles. Color of all the samples darkened after sintering, which indicates sintering of the YSZ crystalline with incorporation of the sintering promoter. The sintered coupon looks flat and uniform. By varying loading of the coated materials, the membrane of different thickness was obtained. No crack, delamination, or deformation occurred among all the thirteen samples of thickness ranged from 2 to 23 μm. After sintering, the ceramic coating layer adhered to the porous Ni support sheet as an integrated body. The sintered membrane was soaked in a 50 wt. % KOH solution and no crack occurred. Electrical conductivity of the ceramic coating was tested. The results show that the coating layer does not present any electrical conductivity when its thickness is at about or above 10 μm, which suggests that the metallic surface was fully insulated by the ceramic coating.

[0061] YSZ is a refractory material. Formation of porous YSZ membranes on a ceramic support typically requires sintering temperatures above 1000° C. in air or oxygen-containing gas environment. It has been very difficult to sinter YSZ coatings on a porous metal support structure due to the limitation of the metallic material properties. In an oxygen-containing gas environment, the metallic structure would be oxidized and destroyed at high temperatures. Even in an oxygen-free gas environment, the metallic structure can experience dramatic shrinkage when heated at high temperatures, which would result in cracks and/or delamination of the ceramic coating layer. This example demonstrates the feasibility to prepare thin (<40 μm) porous ceramic membranes or coatings on the porous metal-based support structures through reactive processes under controlled temperature and gas flow profiles in a continuous reactor system.

[0062] The YSZ coating dramatically reduces surface pore sizes. Micro-structures of the porous metal sheet coated with the 200 nm YSZ particles are shown in FIGS. **13**A-C at different magnification (2,500; 15,000; 50,000). Compared to the surface pore structure of the metal support sheet (FIG. **11**), the YSZ coating surface looks much smoother and comprises pores in the tens of nm. The surface pore size is reduced by about an order of magnitude relative to the pores in the metal sheets. Under 50,000× magnification, FIG. **13**C shows that the neck-to-neck sintering of the YSZ crystalline grains occurred. Uniform distribution of the promoter (NiO) is revealed by elemental mapping of Zr, Ni, and Y in FIG.

13D (5,000× magnification). No segregated NiO phase was found. The surface pore size was further reduced by applying the 50 nm YSZ coating on the 200 nm coating. Compared to FIG. **13**C, FIG. **14**A (50,000× magnification) shows that large pores between the 200 nm crystalline grains were substantially filled by the 50 nm YSZ crystalline and finer surface pores were formed. The elemental mapping at 5000× magnification in FIG. **14**B also confirms uniform distribution of Zr, Y, and Ni elements. The NiO promoter was incorporated into the YSZ crystalline after sintering.

Example III: Formation of Micro-Porous Carbon Coating on the Thin Metal Sheet-Based Support

[0063] The carbon precursor was coated on the porous Ni sheet support by vacuum filtration. The coating material and loading density for four samples are listed in Table 4. The support sheet was cut into 3.5 cm×5.5 cm coupons. The coating was deposited on the coupon in 3 cm×5 cm region. In first two samples, phenol-formaldehyde thermosetting (PFT) resin solution in ethanol was used. The 50 nm/200 nm YSZ-coated porous Ni sheet was as used for sample **1** and the bare porous Ni sheet of about 50 μm thickness was used for sample **2** to see the impact of the support surface on formation of micro-porous carbon membranes. The phenol-formaldehyde thermoplastic resin (PFTP) solution in ethanol was used for samples **3** and **4**. The support used for sample **3** was the porous Ni sheet grown with a NaA-type zeolite membrane. For comparison, the bare Ni sheet was used as a support for sample **4**. The coated sample was dried to remove all the solvent and volatile component. The surface loading density of the carbon precursor, i.e., phenol-formaldehyde resin, is listed in Table 3. The dried samples were loaded into a tunnel reactor with continuous nitrogen gas flow. The samples were heated from room temperature to 700° C. and held at 700° C. for 1 h to remove oxygen and a fraction of carbon from the carbon precursor, and to form micro-porous carbon structures. The last column in Table 4 shows that weight loss of the coating material was greater than 50% for all the samples. The morphology changes are shown in FIG. **15**. After the reaction, a continuous porous carbon layer was formed on both sample **1** and sample **2**. Sample **1** remained flat, while sample **2** curled slightly. Significant curling occurred with sample **3**. No continuous carbon film was formed on sample **4**, due to an insufficient amount of coating, penetration into the support pore, and/or excessive decarbonization.

TABLE 4

Carbon coating on porous metal support sheet

Sample No.	Coating solution	Support	Overall coating thickness on the metal sheet, μm	Coating density of carbon precursor, mg/cm^2	Carbon precursor loading, wt. % of support sheet	Carbon coating weight loss, wt. %
1	35 ml, 2 wt. % of PFT	50 nm/200NM YSZ-coated Ni sheet	39	0.7	1.9%	−65%
2	3 ml of 20 wt. % of PFT	Bare Ni Sheet	27	1.1	2.4%	−63%
3	35 ml of 2 wt. % of PFTP	NaA-type zeolite grown on the metal sheet	17	0.4	1.0%	−54%
4	35 ml of 2 wt. % of PFTP	Bare Ni Sheet	13	0.9	2.2%	−83%

[0064] The example demonstrates the feasibility to form new micro-porous structures from a dense or less porous coating precursor on the porous metal support structure by reaction in flowing gas under a certain temperature profile.

Example IV: Formation of Micro-Porous Structures Inside Pores of a Porous Metal Support

[0065] A porous Ni sheet of about 50 um thickness was used as a support. Three support coupons were impregnated with 0.1M iron nitrate, cobalt nitrate, and Ni nitrate solutions, respectively. After drying, the metallic grains inside pores of the three metal support sheets were functionalized by respective Fe, Co, and Ni catalyst. The functionalized coupons were placed inside a tunnel reactor. The reactor was first purged by nitrogen gas flow and then by hydrogen gas flow. The reactor was heated to 650° C. in continuous hydrogen gas flow. At 650° C., the hydrogen gas flow was switched to ethanol/nitrogen gas flow. The sample was exposed to the ethanol/nitrogen gas flow for about 10 min. Carbon nanotubes (CNT) were grown inside the pores of the metal support sheet. FIG. **16** shows morphologies of the coupons before and after the reaction. The functionalized porous Ni sheets looked like the original nickel sheet, because most catalyst was fixed inside the pores. All the three coupons looked black after the reaction growth. The sheets basically remained flat but with slight deformation on the edges. Under the same conditions, different amounts of the CNT loading were obtained with the three catalysts. The Ni catalyst resulted in the largest CNT loading. The presence of CNT inside the pores was confirmed by SEM analysis. FIGS. **17**A and **17**B show the surface textures of the porous Ni sheet with CNT grown on the Fe catalyst seeding (sample **1** in FIG. **16**B) under 3,000 and 20,000× magnification, respectively. It can be seen that the pores of the nickel support sheet remained intact, but CNT features were added inside the pores. The Fe catalyst promoted formation of

CNT of 50-100 nm diameter and several micrometer long Similar CNT growth was promoted by the Co catalyst. FIG. **17**C shows the surface texture of the porous Ni sheet with CNT grown on the Co seeding (sample **2** in FIG. **16**B) under 30,000× magnification. The Ni catalyst promoted growth of CNT of smaller diameter (30-50 nm). The analysis of the fractured wall confirmed growth of the CNT throughout the support sheet thickness. FIGS. **17**D, **17**E show the fractured porous Ni sheet wall with CNT growth on the Ni sheet (sample **3** in FIG. **16**B) under 1,600 and 20,000× magnification, respectively. This example demonstrates the feasibility to grown smaller porous structures inside the pore of a porous metal support structure through gas/solid reactions in continuous gas flow.

[0066] While several embodiments of the present invention have been shown and described, it will be apparent to those skilled in the art that many changes and modifications may be made without departing from the invention in its broader aspects. The appended claims, therefore, are intended to cover all such changes and modifications as they fall within the true spirit and scope of the invention.

[0067] The following references are hereby incorporated by reference in their entirety.

[0068] Ruben Samuel "Process for producing microperforated stainless steel sheets" U.S. Pat. No. 3,352,769A (Original Assignee: Ruben Samuel; Priority date: 1967 Jan. 11). An electrically controlled process for producing microperforated stainless steel which comprises connecting a sheet of stainless steel having a thickness between approximately 0.0005" and 0.005", containing intergranular iron chromium precipitates and containing as essential elements a preponderance of iron and a lesser but significant amount of chromium as the anode in an electrolytic cell having a non-polarizing electrolyte and a cathode and discharging direct current through said cell so as to anodically dissolve intergranular iron chromium precipitates in said sheet and to thereby produce a multiplicity of light transmitting microperforations through said sheet, the microperforations being primarily due to electrochemical action.

[0069] Anthony J. Vaccaro, Kenneth J. Gregg, Daniel W. Gibbons, Janet S. Gregg, John R. Griesser "Conductive metal porous sheet production" U.S. Pat. No. 5,738,907A (Current Assignee: Stork Screens BV; Original Assignee Eltech Systems Corp; Priority date: 1995 Aug. 4). A porous product, typically a metal foam sheet, is produced as a tailored, engineered product. Thus, an engineered product can be produced which, for example, as an open-cell metal foam prepared from a polymeric foam can have conductivity, both thermal and electrical, as well as strength and ductility, tailored for greater uniformity and performance.

[0070] Hirofumi Sugikawa "Method of manufacturing a metal sheet" U.S. Pat. No. 5,850,591A (Current Assignee: Katayamo Special Industries Ltd; Original Assignee: Katayamo Special Industries Ltd; Priority date: 1996 Apr. 19). A method of manufacturing a porous metal sheet having pores forming a pattern, comprising the steps of supplying metal powders to a peripheral surface, of at least one pattern roller of a pair of rollers, on which a pattern including a large number of concaves is formed; dropping metal powders to the concaves and accumulating metal powders on the peripheral surface of the pattern roller except the concaves; and rolling directly the metal powders accumulated on the peripheral surface of the pattern roller by rotating a pair of the rollers. It is preferable to laminate porous metal sheets or solid metal sheets manufactured by a method other than the above-described method on the metal sheet manufactured by the above-described method.

[0071] 李卫杰 杨谦 杨进 "Horizontal continuous annealing furnace for annealing titanium strips and steel strips" CN203569154U (Original Assignee: 中冶南方(武汉) 威仕工业炉 有限公司; Priority date: 2013 Nov. 8). The utility model relates to a horizontal continuous annealing furnace for annealing titanium strips and steel strips. The horizontal continuous annealing furnace comprises a heating section, a transition section and a cooling section, wherein sealing systems are respectively arranged before the heating section and after the cooling section, and a protective atmosphere in all sections of the furnace is communicated; . . . . The horizontal continuous annealing furnace can be used for continuous annealing of the titanium strips and the steel strips so as to obtain the annealed titanium strips and the steel strips with uniform structures and performances and good surface quality.

[0072] Teruhisa Nakamura "Seal assembly for thermal treatment furnaces using an atmospheric gas containing hydrogen gas" U.S. Pat. No. 5,693,288A (Current Assignee: Nisshin Steel Co Ltd; Priority date: 1994 Jun. 24). A seal assembly located at an entrance or exit of a heat treatment furnace for heat treating a continuously fed metallic strip using an atmospheric gas containing hydrogen gas as a furnace gas and including an elastic rotating roll which is engaged with an elastic pad fixed on a surface of a seal plate and the metallic strip to seal an inside of the furnace against outside air, wherein elastic members are provided in through-holes formed through a side plate of a furnace wall at positions corresponding to both side edges of the elastic pad and elastic member-moving mechanisms are provided for engaging the elastic members with the sides of the elastic pad.

[0073] Rüdiger Dr.-Ing. Conrad "Process for annealing metallic work pieces in a continuous furnace" EP0311030A1 (Current Assignee: Linde AG Original; Priority date 1987 Oct. 7). Annealing processes in which blanketing gas atmospheres are used which contain nitrogen and hydrogen, are known, for example cracked ammonia gas. During annealing in continuous furnaces, so-called white dust forms, which precipitates in the cooling zone and especially in the heat exchangers arranged therein, which causes the entire continuous annealing furnace to be closed down. The formation of white dust is considerably reduced by using pure hydrogen as the blanketing gas in annealing.

1. A method for producing metal-based micro-porous structures comprising:

continuously feeding a solid green part and a gas flow into a tunnel reactor having an aspect ratio greater than 2, wherein the solid green part has a characteristic diffusion mass transfer dimension less than 1 mm and a gas in the gas flow is substantially free of oxidants; and

chemically reacting the gas in the gas flow and the green part under a predetermined temperature profile along a length of the tunnel reactor for a sufficient time to convert the green part into a solid product having pore sizes in a range of 0.3 nm to 5 μm.

2. The method of claim **1**, wherein the solid green part has a residence time in the tunnel reactor greater than 10 minutes.

3. The method of claim **1**, wherein the green part and the gas flow move counter-currently to each other inside the tunnel reactor.

4. The method of claim **1**, wherein the predetermined temperature profile comprises increasing a temperature of the green part to a reaction temperature greater than 500° C. for complete conversion of the green part into the solid product and decreasing a temperature of the solid product from the reaction temperature to below 300° C. at an exit of the tunnel reactor.

5. The method of claim **1**, wherein:

the green part comprises a sheet having a thickness less than 500 μm, metal oxide particles less than 5 μm, a pore former, and an organic additive;

the gas in the gas flow comprises hydrogen gas; and

wherein chemically reacting the gas in the gas flow and the green part comprises:

removing the pore former and organic binders; and

reducing and sintering the metal oxide particles into a porous structure comprising metallic grains.

6. The method of claim **1**, wherein:

the green part comprises a ceramic coating on a porous metal-based support structure, the porous metal-based support structure having pore sizes in a range of 0.1 to 5 μm; and

the ceramic coating comprises:

a thickness less than 40 μm;

metal oxide or ceramic particles having sizes smaller than the pore sizes of the porous metal-based support structure;

organic additives; and

sintering promoters.

7. The method of claim **1**, wherein:

the green part comprises a carbon-containing coating on a porous metal-based support structure having a pore size in a range of 0.1 to 5 μm;

the carbon-containing coating comprises a thickness less than 40 μm; and

the carbon-containing coating comprises oxygen.

8. The method of claim **1**, wherein:

the green part is a functionalized coating;

the gas in the gas flow comprises a silicon containing compound; and

the functionalized coating comprises a porous metal oxide coating having a pore size less than 0.1 μm and a thickness less than 40 μm.

9. The method of claim **8**, wherein the functionalized coating is located on a porous metal-based support structure having a pore size in a range of 0.1 to 5 μm and the silicon containing compound reacts with the functionalized coating to form porous silicon carbide or silica structures.

10. The method of claim **1**, wherein:

the green part comprises a functionalized coating comprising a transition metal catalyst deposited inside pores of a porous metal-based support structure having pore size in a range of 0.1 to 5 μm; and

the gas in the gas flow comprises a carbon precursor gas which reacts to form carbon nanotube-type porous structures inside the pores of the porous metal-based support structure.

11. A method of forming a porous structure, the method comprising:

preheating a green part in a preheating section of a furnace having a first temperature profile;

heating the green part in a reaction and sintering section of the furnace having a second temperature profile different than the first temperature profile; and

during the heating of the green part, reacting a reactant gas with the green part to convert the green part into the porous structure.

12. The method of claim **11**, further comprising:

cooling the porous structure in a cooling section of the furnace having a third temperature profile different than the first temperature profile and the second temperature profile.

13. The method of claim **12**, wherein the first temperature profile comprises a temperature increase along a first length of the furnace to a temperature in a range from 200° C. to 450° C., the second temperature profile comprises a temperature increase along a second length of the furnace to a temperature in a range from 500° C. to 1300° C., and the third temperature profile comprises a temperature decrease along a third length of the furnace to a temperature below 300° C.

14. The method of claim **13**, wherein the temperature increase along the first length of furnace comprises a first rate of change, the temperature increase along the second length of furnace comprises a second rate of change greater than the first rate of change, and the temperature decrease along the third length of furnace comprises a third rate of change greater than the second rate of change.

15. The method of claim **11**, wherein the reacting of the reactant gas with the green part comprises:

reacting the reactant gas with a pore former in the green part to remove the pore former; and

reacting the reactant gas with a metal precursor in the green part to reduce the metal precursor to metallic grains.

16. The method of claim **11**, further comprising:

continuously moving the green part through the furnace, wherein the reacting of the reactant gas with the green part comprises reacting the reactant gas with the green part as the reactant gas flows in the furnace in a direction that is opposite a moving direction of the green part.

17. The method of claim **11**, further comprising:

before the preheating of the green part, supplying the green part to an inlet gas exchange chamber and supplying the inlet gas exchange chamber with an inert gas to remove oxygen from the inlet gas exchange chamber.

18. The method of claim **11**, further comprising:

supplying the porous structure to an outlet gas exchange chamber and supplying the outlet gas exchange chamber with an inert gas to remove the reactant gas from the porous structure.

19. The method of claim **11**, further comprising:

continuously exhausting from the furnace a product gas produced by the reacting of the reactant gas with the green part.

20. A method of forming a porous structure, the method comprising:

supplying a green part comprising a metal precursor and a pore former to an inlet gas exchange chamber and supplying the inlet gas exchange chamber with an inert gas to remove oxygen from the inlet gas exchange chamber;

preheating the green part in a preheating section of a furnace having an aspect ratio greater than 2, wherein the preheating section includes a first temperature profile in which a temperature increases along a first length of the furnace to a temperature in a range from 200° C. to 450° C.;

heating the green part in a reaction and sintering section of the furnace having a second temperature profile in which a temperature increases along a second length of the furnace to a temperature in a range from 500° C. to 1300° C.;

during the heating of the green part, reacting a reactant gas with the green part to convert the green part into the porous structure having pore sizes in a range of 0.3 nm to 5 μm, wherein the reacting of the reactant gas with the green part comprises:

reacting the reactant gas with the pore former in the green part to remove the pore former; and

reacting the reactant gas with the metal precursor in the green part to reduce the metal precursor to metallic grains;

cooling the porous structure in a cooling section of the furnace having a third temperature profile in which a temperature decreases along a third length of the furnace to a temperature below 300° C.; and

supplying the porous structure to an outlet gas exchange chamber and supplying the outlet gas exchange chamber with an inert gas to remove the reactant gas from the porous structure.

* * * * *